Elsevier Editorial System(tm) for Progress in Energy and Combustion Science
Manuscript Draft

Manuscript Number:

Title: Transport Properties for Combustion Modeling

Article Type: Review Article

Keywords: transport properties; combustion modeling; intermolecular potential; collision integrals

Corresponding Author: Dr. Nancy J Brown,

Corresponding Author's Institution: University of California

First Author: Nancy J Brown, PhD

Order of Authors: Nancy J Brown, PhD; Lucas Antoine Jean Bastien; Phillip N Price, PhD

Abstract: This review examines current approximations and approaches that underlie the evaluation of transport properties for combustion modeling applications. Discussed in the review are: the intermolecular potential and its descriptive molecular parameters; various approaches to evaluating collision integrals; supporting data required for the evaluation of transport properties; commonly used computer programs for predicting transport properties; the quality of experimental measurements and their importance for validating or rejecting approximations to property estimation; the interpretation of corresponding states; combination rules that yield pair molecular potential parameters for unlike species from like species parameters; and mixture approximations. The insensitivity of transport properties to intermolecular forces is noted, especially the non-uniqueness of the supporting potential parameters. Viscosity experiments of pure substances and binary mixtures measured post 1970 are used to evaluate a number of approximations; the intermediate temperature range $1 < T^* < 10$, where T^* is kT/ε, is emphasized since this is where rich data sets are available. When suitable potential parameters are used, errors in transport property predictions for pure substances and binary mixtures are less than 5 %, when they are calculated using the approaches of Kee et al.; Mason, Kestin, and Uribe; Paul and Warnatz; or Ern and Giovangigli. Recommendations stemming from the review include (1) revisiting the supporting data required by the various computational approaches, and updating the data sets with accurate potential parameters, dipole moments, and polarizabilities; (2) characterizing the range of parameter space over which the fit to experimental data is good, rather than the current practice of reporting only the parameter set that best fits the data; (3) looking for improved combining rules, since existing rules were found to under-predict the viscosity in most cases; (4) performing more transport property measurements for mixtures that include radical species, an important but neglected area; (5) using the TRANLIB approach for treating polar molecules and (6) performing more accurate measurements of the molecular parameters used to evaluate the molecular heat capacity, since it affects thermal conductivity, which is important in predicting flame development.

Electronic Annex

Click here to download Electronic Annex: CoverBrownBastPri.docx

Submitted to Progress in Energy and Combustion Science

Transport Properties for Combustion Modeling

Nancy J. Brown*, Lucas Bastien, and Phillip N. Price

Atmospheric Sciences Department

Environmental Energy Technology Division

Lawrence Berkeley National Laboratory

Berkeley California, 94707

April 5, 2010

*Corresponding author:

Nancy J. Brown, MS 90 K-110, Berkeley California 94720-8108;

njbrown@lbl.gov

510-486-4241 Fax: 510-486-5928

Key Words: transport properties, combustion modeling, intermolecular potential, collision integrals

This work was supported by the Director, Office of Science, Office of Basic Energy Sciences, Chemical Sciences, Geosciences, and Biosciences Division of the U.S., Department of Energy, under contract No. DE-AC02-05CH11231.

ABSTRACT

This review examines current approximations and approaches that underlie the evaluation of transport properties for combustion modeling applications. Discussed in the review are: the intermolecular potential and its descriptive molecular parameters; various approaches to evaluating collision integrals; supporting data required for the evaluation of transport properties; commonly used computer programs for predicting transport properties; the quality of experimental measurements and their importance for validating or rejecting approximations to property estimation; the interpretation of corresponding states; combination rules that yield pair molecular potential parameters for unlike species from like species parameters; and mixture approximations. The insensitivity of transport properties to intermolecular forces is noted, especially the non-uniqueness of the supporting potential parameters. Viscosity experiments of pure substances and binary mixtures measured post 1970 are used to evaluate a number of approximations; the intermediate temperature range $1 < T^* < 10$, where T^* is kT/ε, is emphasized since this is where rich data sets are available. When suitable potential parameters are used, errors in transport property predictions for pure substances and binary mixtures are less than 5 %, when they are calculated using the approaches of Kee et al.; Mason, Kestin, and Uribe; Paul and Warnatz; or Ern and Giovangigli. Recommendations stemming from the review include (1) revisiting the supporting data required by the various computational approaches, and updating the data sets with accurate potential parameters, dipole moments, and polarizabilities; (2) characterizing the range of parameter space over which the fit to experimental data is good, rather than the current practice of reporting only the parameter set that best fits the data; (3) looking for improved combining rules, since existing rules were found to under-predict the viscosity in most cases; (4) performing more transport property measurements for mixtures that include radical species, an important but neglected area; (5) using the TRANLIB approach for treating polar molecules and (6) performing more accurate measurements of the molecular parameters used to evaluate the molecular heat capacity, since it affects thermal conductivity, which is important in predicting flame development.

Contents

I. Introduction

I. 1. Background

Transport properties such as viscosity, diffusion, thermal conductivity, and thermal diffusion (the so-called Soret effect) play a critical role in combustion processes just as chemical reactions and their underlying kinetic parameters are essential for combustion modeling; molecular transport is important as well. Flame profile shapes, flame velocities, and pollutant production are all affected by transport properties.

Recent work by Middha et al. [1], Paul and Warnatz [2], Grcar et al. [3], and Brown and Revzan [4] has indicated the need for revisiting the approach to calculating the transport properties required to support combustion modeling. Sensitivity analysis by Brown and Revzan revealed that transport properties and their supporting potential parameters are as important in flame modeling as reaction rates. Accurate flame modeling requires accurate chemical kinetics, transport properties, and thermochemistry.

The combustion modeling community has recognized the importance of improving the modeling of chemical mechanisms associated with the combustion of different fuels, but has not directed similar attention to the treatment of molecular transport. Wakeham et al. [5] adeptly summarize recent efforts in transport research: "there [was] considerable development in both transport property theory and experimentation between 1950 and 1970; between 1970 and 1986, these efforts were extended to more complex molecular systems, and currently the field has stagnated with little new development and is driven by specific application needs."

I. 2. Scope of review

The purpose of this review is to examine current approximations and approaches that underlie the evaluation of transport properties and assess their adequacy for combustion modeling. We evaluate the accuracy of transport properties of pure substances and binary mixtures within the context of the current theoretical and experimental studies archived in the literature, considering the work of Kee et al. [6], Mason, Kestin and their many colleagues [7-11], Paul and Warnatz [2], Ern and Giovangigli [12-18] and the many others who measured and collected specific transport property data at a range of conditions (e.g., NIST data by Lemmon et al. [19]). Also discussed are: the intermolecular potential and its descriptive molecular

parameters; various approaches to evaluating collision integrals; supporting data required for the evaluation of transport properties; the quality of experimental measurements and their importance for validating or rejecting approximations to property estimation; the interpretation of corresponding states; combination rules that yield pair molecular potential parameters for unlike species from like species parameters; and mixture approximations. We focus on the intermediate temperature range $1 < T^* < 10$, where T^* is kT/ε, k is the Boltzmann constant, T is the temperature, and ε is the depth of the potential well that characterizes intermolecular interactions, as we discuss later. This temperature range is where rich data sets are available. We consider higher temperatures for a few species where data exist. The various approaches and approximations are evaluated by comparing calculated viscosities and diffusion coefficients of pure substances and binary mixtures relative to their experimental values. We assume that the validation for calculated viscosities extends to calculated diffusion coefficients since viscosity measurements are more accurate than measurements of diffusion. Thermal conductivity, which is important in flame development, is treated briefly here and will be a subject of a later paper as will thermal diffusion. In the former case, inelastic collisions are often important, and in the latter there is more dependence of the shape function of the molecular potential U(r), where $U(r) = \varepsilon\varphi(r/\sigma)$ where φ is the shape function of the molecular potential.

II. Intermolecular potentials for the calculation of transport properties:

Considerable work has been devoted to the transport properties of rare gases, both as single gases and in mixtures. A central force approximation is adequate for such systems. For more complex molecular systems, the importance of orientation-dependent forces for transport property calculations depends on molecular properties such as dipole moments and on additional phenomena such as internal rotations. Accurate experimentally determined viscosities can be used to validate or challenge various approximations, including those that underlie evaluation of other transport properties.

As discussed in Maitland et al [20], the intermolecular potential can be divided into regions based on the distance between the centers of mass of the interacting molecules. Forces acting at short range are repulsive, and result from the overlap of the molecular wave functions and from symmetry requirements imposed by the Pauli Exclusion Principle. At longer range electrostatic,

induction, and dispersion forces dominate. Long-range electrostatic forces are present when each of the two molecules has a dipole or quadrupole moment, although the latter is not usually important for transport calculations. These forces are often called first-order orientation forces, and, when averaged over orientation with proper weighting, are attractive. Induction forces occur when one or both molecules have a dipole moment: the dipole moment of one molecule distorts the electron charge distribution of the other molecule, and produces an induced dipole. Induction forces between the inducing and induced dipole are often called second-order forces. They depend on orientation, and are attractive when properly weighted and averaged over orientation. Dispersion forces are always present for two molecules and are the only type of attractive force at longer range for two molecules when neither has a dipole moment. The electron density oscillates in time and space as a result of the constant motion of the electrons of each molecule. Dispersion energy results from the correlation between electronic density fluctuations in the two molecules. The induction force is usually the weakest of the three.

The representation of the three types of potential energy used for most transport calculations is based on simplifying approximations. We first consider a pair of polar molecules and treat the system as two interacting linear charge distributions. The leading term is the dipole-dipole interaction term

$$U = \frac{\mu\mu'}{4\pi\varepsilon_0 r^3}\xi(\Theta_1\Theta_2\Phi) \tag{1}$$

where

$$\xi(\Theta_1\Theta_2\Phi) = 2\cos\Theta_1\cos\Theta_2 - \sin\Theta_1\sin\Theta_2\cos\Phi \tag{2}$$

describes the orientation dependence of the energy, and θ_1 is the angle that the vector associated with intermolecular distance makes with the vector associated with intramolecular distance. The average energy over all orientations can be calculated assuming the two molecules are gaseous and free to rotate. The probability of observing a configuration having a particular energy is proportional to a Boltzmann factor. This leads to larger weighting factors for configurations of negative energy, renders the average negative and the potential energy attractive, and yields:

$$\langle U_{el}\rangle = -\frac{2}{3}\frac{\mu^2\mu'^2}{(4\pi\varepsilon_0)^2 kTr^6} \tag{3}$$

Since the average value of the potential energy decreases as 1/T, its importance is diminished at the higher temperatures associated with combustion.

The induction force depends on the existence of a permanent dipole in at least one of the two molecules, and is also attractive. The induction energy associated with a simple molecule with a permanent dipole interacting with another molecule with static polarizability α' is often approximated as

$$U_{ind} = \frac{1}{2}\alpha' \frac{\mu^2(}{r^6} \frac{3\cos^2\Theta + 1)}{(4\pi\varepsilon_0)^2} \tag{4}$$

Averaging this over all orientations with Boltzmann weighting factors yields an average induction energy of:

$$\langle U_{ind} \rangle = \frac{\mu^2 \alpha'}{(4\pi\varepsilon_0)^2 r^6} \tag{5}$$

Dispersion forces are always present between molecules regardless of whether or not the interacting molecules have permanent dipoles. Dispersion forces are attractive, and include terms in r^{-6}, $r^{-8,}$ and r^{-10}; however, in most cases only r^{-6} is relevant because the higher-order terms are small by comparison. Using a simplified Drude model [21], where it is assumed that each molecule consists of one negatively charged and one positively charged particle, the energy arising from two oscillating dipoles, treated like harmonic oscillators, is given by:

$$U_{dis} = -\frac{3}{4} \frac{\alpha^2 \hbar \omega_0}{(4\pi\varepsilon_0)^2 r^6} \tag{6}$$

The origin of the dispersion energy in this case is purely quantum mechanical, and arises from the zero point energy of the oscillators.

These simple models justify the assumption that the attractive energy at long range behaves like $1/r^6$. The approximate energy for the long-range forces is:

$$U = -\frac{1}{(4\pi\varepsilon_0)^2 r^6} [\frac{2}{3} \frac{\mu^2 \mu^2}{kT} + 2\mu^2 \alpha + \frac{3}{4} \alpha^2 \hbar \omega_0] \tag{7}$$

Forces that act at shorter range result from the repulsion of incompletely screened nuclei, from the repulsion between electrons associated with the two molecules, and, less obviously, from the Pauli Exclusion Principle which imposes certain symmetry requirements on the

wavefunctions. The short range forces therefore include the well-known Coulomb, exchange, and overlap integrals; all of these forces are repulsive. The multipole expansion used to represent the longer-range forces does not converge when the electron clouds of the two molecules overlap.

Although valence bond theory is not the most successful for treating short range forces, it does illustrate the essential physics, and it can be used to examine the interaction of two H atoms at close range to explore the physics of this interaction and to understand why the repulsive force is often represented by a $1/r^n$ or an $\exp(-\beta r)$ form. In the $^1\Sigma^-$ repulsive state of H_2, the potential energy at moderately short range indicates that it behaves as $\exp(-\beta r)$ at shorter distance and r^{-n} at larger distances. It is easier to obtain an accurate representation at very short range where there is considerable overlap of the wavefunctions of the two molecules and at longer range where there is little, if no, overlap. The intermediate range, where overlap persists and the potential energy remains repulsive is a challenge. The interaction energy in this range is not terribly large, and is evaluated numerically as the difference between the energy of the total system at a series of center-of-mass separations and the energy of the two atoms or molecules at infinite separation. Considerable accuracy is lost as a result of the subtraction.

In practice, for calculating transport properties it is not necessary to calculate the intermolecular potential in detail. Ultimately, what is needed to calculate transport properties is the value of collision integrals that are a function of the intermolecular potential but are not highly sensitive to its details. Approaches to calculating the collision integrals include using a simple functional form for the potential as a basis for the calculation, or using an empirically determined expression for the collision integrals themselves (see Mason and Uribe [11] for example).

The most commonly used potential is the Lennard-Jones (L-J) 12-6 potential, defined as:

$$U(r) = 4\varepsilon\left[\left(\frac{\sigma}{r}\right)^{12} - \left(\frac{\sigma}{r}\right)^{6}\right] \tag{8}$$

The L-J potential requires only two parameters to characterize interacting molecules: a well depth ε (which is the maximum attractive energy) and a characteristic distance σ (which is the distance at which the potential is zero). Various modifications of the L-J potential have been proposed, most of them involving the introduction of additional molecular parameters, but the L-

J potential works remarkably well. Calculation of the collision integrals with this potential yields values that are nearly identical with the empirically determined values of Mason and Uribe, as shown in Figure 1.

In a more modern vein, calculations of transport properties supported by ab initio potential energy surface calculations have been accomplished by a group of investigators from NASA Ames. An early contribution was by Stallcop et al. [22], who evaluated transport cross sections and collision integrals for the H + N_2 system. The potential energy system was calculated using a complete active space self-consistent field/externally contracted configuration interaction (CASSCF/CCI) method. A long range dispersion energy approximated with a damping function and a Born-Mayer potential repulsive potential combined with the ab initio results was used to evaluate the transport properties. Good agreement was obtained with experiment for the diffusion and viscosity coefficients at room temperature and atmospheric pressure.

Partridge et al. [23][24] computed a potential energy surface and transport coefficients for H + H_2 using an ab initio approach at short internuclear distances and filling in the intermediate distance between 4.0 and 8-10 atomic units with a more empirical approach. At the larger separations their work showed that using a Born Mayer potential for the repulsive energy and treating the attractive energy as dispersion energy, computed with the damping function approach of Tang and Toennies [25], worked well. Their surface was used to compute diffusion and viscosity coefficients by treating the scattering with the Infinite Order Sudden Approximation (IOSA). They demonstrated the success of the IOSA by comparing its collision integrals with collision integrals computed using a close coupling result. The results for H + H_2 viscosity and diffusion coefficients gave good agreement with experiment.

Other systems treated by the group that has relevance to combustion are H+ O_2 [26]; H + H, H+ H_2, and H_2 + H_2 [24][27]; N_2 + N_2 [28]; N_2 + He, N_2 + H_2, N_2 + N_2 [29]; C_2 and CN [30]; H_2 + N and N_2 + N [31]. Especially of interest for combustion modeling is the Aufbau method they developed for determining dispersion coefficients of effective potential energies from the data associated with other interactions. For example, using the potential for H_2 + H_2 and N_2 + H_2, they use the Aufbau method, which is akin to a combing rule, to infer the potential for N_2 + N_2.

III. Evaluation of Transport Properties

Transport properties used in combustion modeling – diffusion, viscosity, thermal conductivity, and thermal diffusion – are developed from kinetic theory using classical mechanics of binary collisions as described in Hirschfelder, Curtis, and Bird [32]. According to Mason and Uribe [11], classical treatments are perfectly adequate for molecular systems in the regime, T* > 1 for viscosity and diffusion.

The deflection function contains the information about the collision dynamics that is required to calculate cross sections relevant for the evaluation of transport properties: it gives the relative angle between interacting molecules after they collide, as a function of the collision velocity and impact parameter. The deflection function, $\chi(g,b)$, is given by:

$$\chi(g,b) = \pi - 2b\int_{r_m}^{\infty} \frac{dr/r^2}{\sqrt{1-\frac{b^2}{r^2}-\frac{U(r)}{\frac{1}{2}\mu g^2}}} \tag{9}$$

where r is the radial distance, b the impact parameter, r_m the distance of closest approach, U(r) is the intermolecular potential, μ the reduced mass, and g is the relative velocity. $\chi(g,b)$ is used to evaluate a cross section as:

$$Q^{(l)}(g) = 2\pi\int_0^{\infty}\left[1-\cos^{l}(\chi)\right]bdb \tag{10}$$

which is weighted and averaged over a Boltzmann distribution to yield a collision integral:

$$\Omega^{(l,s)}(T) = \sqrt{\frac{kT}{2\pi\mu}}\int_0^{\infty} e^{-\gamma^2}\gamma^{2s+3}Q^{(l)}(g)d\gamma \tag{11}$$

where

$$\gamma^2 = \frac{\mu g^2}{2kT} \tag{12}$$

The transport properties are developed from kinetic theory as functions of the collision integrals $\Omega^{(l,s)}$ and certain functionals. The collision integral appropriate for diffusion is obtained when *l* and *s* each equal 1, and for viscosity and thermal conductivity the (2,2) collision integral is needed.

It is customary to work with reduced collision integrals obtained by normalizing the collision integrals by the value they would have if the molecules were rigid spheres of diameter σ_{ij}. (σ_{ij} is the intermolecular separation at which the potential equals zero.) Thus:

$$\Omega_{ij}^{(l,s)*}\left(T_{ij}^{*}\right)=\frac{\Omega_{ij}^{(l,s)}(T)}{\frac{(s+1)!}{2}\left[1-\frac{1+(-1)^{l}}{2(1+l)}\right]\pi\sigma_{ij}^{2}} \tag{13}$$

Reduced collision integrals are functions of the reduced intermolecular pair potential $U_{ij}^{*}\left(r_{ij}^{*}\right)$:

$$U_{ij}^{*}\left(r_{ij}^{*}\right)=\frac{U_{ij}\left(r/\sigma_{ij}\right)}{\varepsilon_{ij}} \tag{14}$$

where ε_{ij} is the well depth of the interacting i and j molecules, and T* = kT/ ε_{ij}. The first order Chapman-Enskog solution and the second order Kihara solution of the Boltzmann equation for the pure species viscosities η are given by the following expressions:

$$[\eta]_{1}(T)=\frac{5}{16}\sqrt{\frac{mk_{B}T}{\pi}}\frac{1}{\sigma^{2}\Omega^{(2.2)*}\left(T^{*}\right)} \tag{15}$$

$$[\eta]_{2}(T)=f_{\eta}[\eta]_{1}(T) \tag{16}$$

where

$$f_{\eta}\left(T^{*}\right)=1+\frac{3}{196}\left(8E^{*}-7\right)^{2} \tag{17}$$

and where the notation $[\eta]_i$ indicates the i^{th} order approximation of the transport property η. Higher order approximations differ from first order by 1 to 2%. Functionals of collision integrals are used for calculating higher order approximations to the transport properties of interest as well as multi component properties; four of these are:

$$A_{ij}^{*}=\frac{\Omega_{ij}^{(2.2)*}}{\Omega_{ij}^{(1.1)*}};B_{ij}^{*}=\frac{5\Omega_{ij}^{(1.2)*}-4\Omega_{ij}^{(1.3)*}}{\Omega_{ij}^{(1.1)*}};C_{ij}^{*}=\frac{\Omega_{ij}^{(1.2)*}}{\Omega_{ij}^{(1.1)*}};E_{ij}^{*}=\frac{\Omega_{ij}^{(2.3)*}}{\Omega_{ij}^{(2.2)*}};F_{ij}^{*}=\frac{\Omega_{ij}^{(3.3)*}}{\Omega_{ij}^{(1.1)*}} \tag{18; 19; 20; 21; 22}$$

The value f_{η} and all ratios of collision integrals, are functions of T*. For multicomponent mixtures with υ components (and binary mixtures for diffusion), the first order solution of the Boltzmann equation gives:

$$\left[\eta_{mix}\right]_1 = \frac{\begin{vmatrix} H_{11}^{00} & H_{12}^{00} & \cdots & H_{1\nu}^{00} & x_1 \\ H_{21}^{00} & H_{22}^{00} & \cdots & H_{2\nu}^{00} & x_2 \\ \vdots & \vdots & \ddots & \vdots & \vdots \\ H_{\nu 1}^{00} & H_{\nu 2}^{00} & \cdots & H_{\nu\nu}^{00} & x_\nu \\ x_1 & x_2 & \cdots & x_\nu & 0 \end{vmatrix}}{\begin{vmatrix} H_{11}^{00} & H_{12}^{00} & \cdots & H_{1\nu}^{00} \\ H_{21}^{00} & H_{22}^{00} & \cdots & H_{2\nu}^{00} \\ \vdots & \vdots & \ddots & \vdots \\ H_{\nu 1}^{00} & H_{\nu 2}^{00} & \cdots & H_{\nu\nu}^{00} \end{vmatrix}} \tag{23}$$

Where:

$$H_{ii}^{00} = \frac{x_i^2}{\left[\eta_i\right]_1} + \sum_{\substack{k=1 \\ k\neq i}}^{\nu} \frac{2x_i x_k}{\left[\eta_{ik}\right]} \frac{m_k}{\left(m_i + m_k\right)^2} \left(\frac{5m_i}{3A_{ik}^*\left(T^*\right)} + m_k \right) \tag{24}$$

$$H_{\substack{ij \\ i\neq j}}^{00} = \frac{2x_i x_j}{\left[\eta_{ij}\right]_1} \frac{m_i m_j}{\left(m_i + m_j\right)^2} \left(\frac{5m_i}{3A_{ij}^*\left(T^*\right)} - 1 \right) \tag{25}$$

$$\left[\eta_{ij}\right]_1 = \frac{5}{16}\sqrt{\frac{m_{ij}k_B T}{\pi}} \frac{1}{\sigma_{ij}^2 \Omega_{ij}^{(2.2)^*}\left(T_{ij}^*\right)}; m_{ij} = \frac{2m_i m_j}{\left(m_i + m_j\right)} \tag{26; 27}$$

where m_k is the molar mass of the molecule k and x_k is its mole fraction. η_{ij} is the interaction viscosity, which represents the viscosity of a hypothetical pure gas whose molecules have a mass m_{ij} that is twice the reduced mass of species i and j, and which interact through an intermolecular potential energy U_{ij} with scaling parameters σ_{ij} and ε_{ij}. Methods of determining the scaling parameters are discussed in a later section.

IV. Measurements

Experiments are needed both to test the formalism described above and to determine the molecular parameters for the interacting species. In this section, we answer the following questions related to experiments: What data are most suited for determining the accuracy of calculated results for the various transport properties, and how accurate are the available data?

IV. 1. Viscosity

The prevailing wisdom, documented in many papers, is that viscosity data are most suitable for evaluating the accuracy of calculations and for establishing the relationship between the potential parameters and the transport properties. Advances in the measurements of transport properties are discussed in an excellent review by Wakeham et al. [5]. Another very important source of information in this area is the work of Kestin and Wakeham [33].

Below, we discuss a number of comparisons between measured and calculated viscosity coefficients for pure species and for binary mixtures of unlike species. Initially we consider the temperature range commensurate with $1 < T^* < 10.0$ since most of the data are in this range. We briefly summarize the different experimental techniques used to measure viscosity coefficients and their accuracy.

Viscosity is a measure of the tendency of a fluid to dissipate energy (produce entropy) when disturbed from equilibrium by the imposition of a flow field that distorts the fluid at a specific rate. The linear relationship describing this is Stoke's Law. The dissipative mechanism of shear is not coupled directly to heat conduction or to diffusive mass transport. Inevitably feedbacks exist; local temperature gradients, enhanced by the energy dissipation due to shear, create changes in the local density and/or composition that must be accounted for. It is not possible to measure local shear stresses or to determine the accompanying thermodynamic state; hence it is necessary to base viscosity measurement methods on some integral effect and to infer the accompanying state by averaging.

Two kinds of viscometers have been mainly employed in the past: oscillating-body viscometers and capillary-flow viscometers. A major development in these approaches was the creation of models of the flow fields associated with them so that viscosities could be extracted from an analysis of the measurements taken. There exist more modern methods (mainly the vibrating-wire viscometer). Better formulae are needed to describe the relationship between the viscosity and the quantities measured, since these formulae are frequently the largest source of error.

IV. 1. a. Oscillating-body viscometers

An oscillating-body viscometer consists of an axially symmetric body that undergoes torsional oscillation in a fluid. The oscillating system is suspended from an elastic wire and gently rotated to initiate the motion. The change in frequency and damping decrement caused by

the fluid relative to those in a vacuum can be related to viscosity, either directly or indirectly. The use of oscillating-body viscometers leads to great simplicity of design and highly precise measurements. Different designs exist: oscillating disks, cups, cylinders, and spherical viscometers. The error of measurements from an oscillating-body viscometer is less than 0.5%. Kestin et al. [34], measured viscosity of eighteen binary mixtures with an error less than 0.2% using a viscometer where the important elements were machined entirely from quartz. As a cautionary note, measurements prior to 1972 are suspect for all molecules except rare gases because the metal parts in the oscillating body viscometers may have facilitated catalytic reactions that would alter concentrations of the molecules [5].

IV. 1. b. Capillary viscometers

A capillary viscometer is used to measure the difference of pressure observed on a fluid when traveling through a piece of tubing. This method sometimes resulted in less accurate values due to the use of a less than satisfactory representation of the relationship between viscosity and the measured pressure difference. Kestin and Wakeham [33] suggest that all tabulations of viscosity at high temperatures prior to about 1970 obtained with capillarity viscometers should be ignored. The error of later measurements is claimed to be below 0.5%.

IV. 1. c. Vibrating-wire viscometer

This method was developed by Retsina et al. in 1986 [35], and it is based upon the effect of a wire vibrating in a fluid. The wire is under tension and the vibration is usually magnetically induced. Modern studies indicate that the uncertainty is less than 0.5% for certain species (i.e. 0.3 % for N_2 viscosity between 298.15 K and 423.15 K and at pressures up to a maximum of 35 MPa by Seibt et al. [36] and 1% for three natural gas mixtures between 263 K and 303 K and between 5 MPa and 25 MPa by Langelandsvik et al. [37]).

IV. 1. d. Evaluation of measured viscosities

Kestin and Wakeham [33] made a comparison of the experimental viscosity data. The largest difference between any of the experimental results was approximately 0.5%, which was commensurate with the accuracy claimed by the authors. Together with modern measurements and more accurate descriptions of the flow fields associated with the various instruments, it is

possible to choose data that have errors less than 0.5%. All the comparison with experiment made in this study use data of this quoted accuracy.

IV. 1. e. Bulk viscosity

The bulk viscosity of polyatomic gases is directly related to inelastic collisions, and there have not been recent experimental studies of these. Earlier measurements of relaxation phenomena were performed with sound absorption and shock tubes for rotational and vibrational relaxation. Since potential energy surfaces and the dynamics calculations associated with evaluating relaxation rates are a great deal more accessible than in the 70s, they could be used to evaluate the importance of the inelastic collisions in molecular transport.

IV. 2. Diffusion

Diffusion is more difficult to measure than viscosity, and is subject to larger errors. Measurements are frequently made using a two-bulb method whereby two bulbs, each with a different composition of two gases, are in contact with one another. The composition of gas in one of the bulbs is measured as a function of time. The measured relaxation time is related to the diffusion coefficient and the instrument geometry. Except for rare gas systems, errors in measured diffusion coefficients are around 3%, which is about three to six times larger than the error in viscosity measurements. Relative errors in diffusion are highest near room temperature and lower when $T > 500$ K.

IV. 3. Thermal Conductivity

Measurements of thermal conductivity were subject to considerable errors, especially for fluids at high temperatures, because of the difficulty of separating heat conduction from heat transfer arising from convection. This problem was largely resolved in the late 70s by Haarman [38], who established the transient hot wire technique as the method of choice for measuring thermal conductivity. The temperature rise in a thin platinum wire that is immersed in the fluid of interest is determined as a function of time over a time interval that is short relative to that required for the development of significant convective heat transfer. High quality data on the thermal conductivity of pure gases are still relatively scarce and cover only a narrow temperature range—that is not extensive enough for combustion modeling. The discrepancy between theory

and experiment is approximately 2% near room temperature, and around 8% for temperatures in excess of 500 K.

V. Current Practice for Calculating Transport Properties

V. 1. The TRANLIB approach

Four approaches are used to evaluate transport properties for combustion modeling. Each is based upon the Law of Corresponding States, which is an underlying principle of molecular similarity. Briefly, invoking the two-parameter version implies that plots of the reduced potential energy, (U/ε) versus reduced distance (r/σ) would fall on a universal curve, where the quantity ε is the well depth and σ is the intermolecular separation at zero potential energy. As stated by Mason and Uribe [11] "In retrospect the general principle of corresponding states has proved to be much better than it had often been thought to be in the past. It has a firm basis in statistical mechanics and kinetic theory, and a great range of accuracy if care is taken not to contaminate it with oversimplified models."

Currently, most transport property evaluation in combustion modeling is accomplished with the TRANLIB collection of codes of Kee et al. [39][6] that are incorporated in the CHEMKIN suite of codes. The TRANLIB codes are described in Sandia Report SAND86-8246, which was reprinted in December 1990. Diffusion, viscosity, thermal conductivity, and thermal diffusion are developed from kinetic theory assuming classical mechanics and binary collisions using the approach described in Hirschfelder, Curtis, and Bird [32] (HCB) and discussed earlier in this review.

TRANLIB uses the collision integrals calculated by Monchick and Mason [40] (M & M) that are developed from the Stockmeyer 12-6-3 potential, which is a Lennard-Jones potential to which a dipole-dipole interaction term has been added as in Equation (1). The potential depends on the center-of-mass separation of the two molecules, r; a function $\xi(\Theta_1\Theta_2\Phi_1\Phi_2)$, where the angles serve to define the orientation of the two molecules; the Lennard-Jones parameters; and for polar molecules, on the two dipole moments μ_1 and μ_2. The Stockmeyer potential does not include terms that account for induction, which is instead included by scaling the two Lennard-Jones parameters according to formulae given in Hirschfelder, Curtis, and Bird [32].

In the evaluation of the collision integrals, Monchick and Mason [40] (M&M) assumed that the system is classical and collisions are elastic. They caution that this approximation will not work for the evaluation of thermal conductivity, where inelastic collisions are important, but it should work for diffusion, viscosity, and thermal diffusion. They evaluate the deflection function via equation (9) by assuming that the deflection angle is primarily determined by the interaction at closest approach, and ignore time-dependence of the molecular orientation. This implies that the collisions follow not one but rather a large number of potentials-each associated with a different orientation but having equal weighting factors. They parameterize the collision integrals with respect to $\delta = \frac{1}{4}(\mu^{*2})\ \xi(\Theta_1\Theta_2\Phi)$ where $\mu^{*2} = \mu^2/(\varepsilon\sigma^3)$. By making these assumptions, the trajectory is replaced by one in which values of ξ and δ are fixed, and the deflection function calculation is reduced to a central force problem. The "pure" Lennard-Jones collision integrals are associated with $\delta=0$. Orientation averaged collision integrals are tabulated in Tables IV and V in the M&M paper as a function of T*, and $\delta^{max} = \mu^2/(2\varepsilon\sigma^3)$. Additionally, functionals denoted A* through F* required to compute higher order corrections to the transport properties, are given in Tables VI through X of the same paper.

In TRANLIB, when only one of the molecules is polar, induction is estimated using the formula given in HCB and our Equation (5) for the interaction between a dipole and induced dipole. When only one member of the pair has a dipole moment, a quantity ξ is defined which requires the dipole moment of the polar molecule and the polarizability of the other molecule for its evaluation. The quantity ξ is unity when both molecules are polar or both are not, but when one molecule is polar and the other is not, it is given by

$$\xi = 1 + \frac{\alpha_n^* \mu_p^{*2}}{(4\pi\varepsilon_0)4}\sqrt{\frac{\varepsilon_p}{\varepsilon_n}} \tag{28}$$

where the subscript p denotes the polar molecule and n denotes the non-polar molecule, and

$$\mu_p^{*2} = \frac{\mu_p^2}{\varepsilon_p \sigma_p^3} \tag{29}$$

and

$$\alpha_n^* = \frac{\alpha_n}{\sigma_n^3} \tag{30}$$

Equation (28), and Equations (47)-(48), are in SI units, where ε_0 is the permittivity of free space. For both historical reasons and for convenience, transport properties calculations are often done in cgs units, which, due to a different way of handling electric charge, requires modification of the equations: in cgs units, the $(4\pi\varepsilon_0)$ terms are absent from the equations.

The scaling parameter ξ is used in calculating the well depth and collision diameter:

$$\varepsilon_{jk} = \xi^2 \sqrt{\varepsilon_j \varepsilon_k} \tag{31}$$

and

$$\sigma_{jk} = \xi^{-1/6} \frac{\left(\sigma_j + \sigma_k\right)}{2} \tag{32}$$

Scaling has a large effect on the well depth and little effect on the collision diameter.

There is sometimes disagreement between the TRANLIB code and manual, and the code is more often correct, e.g., the formula for ξ is incorrect in the manual but is correct in the code. The TRANLIB parameter database contains dipole moments for only a few polar molecules (CH_3O, CH_4O, H_2O, NH_3, HFO_n (n=0,8) which is unfortunate, since there are many more polar molecules in the data set that have dipole moments reported in the literature. Problematically, radical species are polar but most are assigned zero dipole moment in the TRANLIB database. The dipole correction is important, and is more significant at lower temperatures; without it, the viscosity of H_20 is too high by 27 % at 300 K, and 18% at 600 K; including the correction reduces the deviation to values less than 5%. The polarizability data are also very sparse: the database has polarizabilities for only ten molecules.

In TRANLIB, thermal conductivity depends on the rotational relaxation collision number (Z_{rot}) and also upon whether the molecule is monatomic, linear or nonlinear, (denoted in the database by LIN = 0,1, or 2, respectively). The TRANLIB package requires 6 parameters for each molecule.

An attractive feature of TRANLIB is that the logarithm of the transport property is fitted to a third order polynomial in the logarithm of the temperature at the beginning of a simulation and this results in considerable computational savings. This is only relevant for mixture approximations and not for a multicomponent treatment. TRANLIB uses the so called mixture approximation of Wilke [41] that was modified by Bird et al. [42] to determine the viscosity of

mixtures. Grcar [43] found an error in the calculation of the pure species thermal conductivity which is only used for mixture approximation calculations. The error is in the subroutine LAMFIT where the constant HELPD is given the value 2.6280E-3, but should be 1.85879E-3.

V. 2. The approach of Mason, Kestin and Colleagues

MKC [7-11] observed that plots of the reduced potential energy (U/ε) versus (r/r_m) did not fall on a universal curve. The so-called two parameter corresponding states principle failed at very low and high temperatures because the shape function, $U(r) = \varepsilon\varphi(r/\sigma)$, was not universal for the rare gases. Mason and Uribe [11] note the remarkable success of the two-parameter corresponding states principle, pointing out that it is quite successful over a broad range of T* because the transport properties are dominated by the effect of the relatively featureless repulsive wall, and that viscosity and diffusion are not very sensitive to anisotropy of the potential. This conclusion was based on advances made in experiments and theory in chemical physics. Advances included an improved knowledge of the intermolecular potential derived from molecular beam scattering experiments (Parson et al. [44][45] and Scoles [46]), better inversion approaches for deducing the potential energy from experiments, improvements in calculating dispersions energies (Tang and Toennies [25]), and better data associated with the spectroscopy of rare gas dimers.

The rather immense activities in the chemical physics community post 1970s resulted in improved van der Waals potential parameters for a number of systems (see for example, McCourt et al., 1995 [47] and 2002 [48]) There were also purported to be better approaches to the combining of potential parameters for pure species to yield values appropriate for binary mixtures.

These various advances motivated MKC to revise their treatment for the calculation of transport properties for dilute gases. They indicate that there are three energy ranges designated by values of T*. In the first region defined by $T^* \leq 1.0$, dispersion forces, frequently described as only including a C^6/r^6 term, dominate, and this is only for rare gases and their mixtures and not polyatomic molecules. The principle of corresponding states is more limited for polyatomic gases for three reasons: the intermolecular forces tend to be more complex, polyatomic gases undergo inelastic collisions, and there is less experimental data. In the second region, $1.0 \leq T^* \leq 10.0$, the Lennard-Jones potential and its two parameters, σ and ε, are required for collision

integral evaluation. Actually, they give expressions for the collision integrals that are determined from fitting expressions for the calculated properties to experimentally determined values. The collision integrals determined in this fashion are nearly identical to those calculated with a Lennard Jones potential using classical mechanics and Equations (9)-(12), as shown by Figure 1. At T* > 10.0, features of the potential are described by an exponential repulsive potential, the so-called Born Mayer potential, $U(r) = U_o\exp(-\rho R)$, are influential, requiring additional length and energy scaling parameters, ρ and U_o, respectively to evaluate collision integrals. The MKC method adds three new parameters per species, and requires five potential parameters for the calculation of the collision integrals. In later papers, Tang and Toennies [25] derived relationships between ε and σ and U_o and ρ that require dispersion coefficients, thus reducing the number of parameters to three for cases not requiring corrections for non- and weakly polar molecules. Potential parameters for the set of molecules reported by MKC were derived from a set obtained for argon, the application of corresponding states, and viscosity data for species of interest.

$T^* \leq 1.0$, for noble gases only:

$$\Omega^{(1,1)^*} = 1.1874\left(C_6/T^*\right)^{1/3}\left[1+\sum_{i=1}^{6} b_i\left(T^*\right)^{i/3}\right] \tag{33}$$

and for all molecules:

$$\Omega^{(2,2)^*} = 1.1943\left(C_6/T^*\right)^{1/3}\left[1+\sum_{i=1}^{6} a_i\left(T^*\right)^{i/3}\right] \tag{34}$$

where

$$a_i = a_{i1} + a_{i2}\left(C_6^*\right)^{-1/3} \tag{35}$$

$$b_i = b_{i1} + b_{i2}\left(C_6^*\right)^{-1/3} \tag{36}$$

The coefficients are given in Table 1.

$1 \leq T^* \leq 10$:

$$\Omega^{(1,1)^*}\left(T^*\right) = \exp\left[\sum_{i=0}^{4} b_i\left(\ln T^*\right)^i\right] \tag{37}$$

$$\Omega^{(2.2)*}\left(T^*\right)=\exp\left[\sum_{i=1}^{5}a_i\left(\ln T^*\right)^{i-1}\right] \tag{38}$$

The corresponding coefficients are given in Table 2.

$T^* \geq 10$:

$$\Omega^{(1,1)*}\left(T^*\right)=\left(\rho^*\alpha\right)^2\left[0.89+\sum_{i=1}^{3}b_{2i}\left(\ln T^*\right)^{-2i}\right] \tag{39}$$

$$\Omega^{(2.2)*}\left(T^*\right)=\left(\rho^*\alpha\right)^2\left[1.04+\sum_{i=2}^{4}a_i\left(\ln T^*\right)^{-i}\right] \tag{40}$$

where $\alpha=\ln\left(U_0^*/T^*\right)$ and:

$$a_i=a_{i1}+\left(-1\right)^i\left(\rho^*\alpha_{10}\right)^{-2}\left[a_{i2}+a_{i3}/\alpha_{10}+\left(a_{i4}/\alpha_{10}\right)^2\right] \tag{41}$$

$$b_i=b_{i1}+\left(-1\right)^i\left(\rho^*\alpha_{10}\right)^{-2}c_i\left[b_{i2}+b_{i3}/\alpha_{10}+\left(b_{i4}/\alpha_{10}\right)^2\right] \tag{42}$$

where $\alpha_{10}=\ln\left(U_0^*/10\right)$.

Numerical values for the coefficients a_{ij} and b_{ij} are given in Table 3.

MKC present empirically derived expressions for collision integrals, $\Omega^{(1,1)*}$ and $\Omega^{(2,2)*}$ based upon viscosity and diffusion measurements for each of three T* ranges for the rare gases. The correlations were extended to a set of polyatomic molecules [9][10] to enable the calculation of collision integrals appropriate for viscosity, diffusion, and thermal conductivity. Polyatomic molecules considered were: N_2, O_2, NO, CO_2, N_2O, CH_4, CF_4, SF_6, C_2H_4, and C_2H_6. The collision integral $\Omega^{(1,1)*}$ was slightly different for the polyatomic molecules while $\Omega^{(2,2)*}$ was the same for rare gases and polyatomic molecules. Errors in measurements are slightly larger for polyatomic molecules: 0.3 to 1.0% for viscosity and up to 5% for diffusion. None of the molecules considered has a particularly strong dipole moment.

V. 3. Dipole Reduced Formalism Method (DRFM) approach

Paul [49] and Paul and Warnatz [2] adopt the approach of MKC for the calculation of collision integrals. They extend the approach to include more complex molecules by scaling the potential parameters to account for dipole-dipole and dipole-induced dipole interactions:

$$\varepsilon_{ij}^{'} = \varepsilon_{ij}\left(1+\chi_{ij}+\Delta_{ij}/kT\right)^{2} \tag{43}$$

$$\sigma_{ij}^{'} = \sigma_{ij}\left(1+\chi_{ij}+\Delta_{ij}/kT\right)^{-1/6} \tag{44}$$

$$V_{ij}^{'} = V_{ij}^{*}\left(1+\chi_{ij}+\Delta_{ij}/kT\right)^{-2} \tag{45}$$

$$\rho_{ij}^{'} = \rho_{ij}^{*}\left(1+\chi_{ij}+\Delta_{ij}/kT\right)^{1/6} \tag{46}$$

where:

$$\chi_{ij} = \frac{\alpha_i\mu_j^2+\alpha_j\mu_i^2}{(4\pi\varepsilon_0)^2 4\varepsilon_{ij}\sigma_{ij}^6} \tag{47}$$

$$\Delta_{ij} = \frac{\mu_i^2\mu_j^2}{(4\pi\varepsilon_0)^2\varepsilon_{ij}\sigma_{ij}^6} \tag{48}$$

The correct expression for collision integral calculations is given in Bzowski et al. [10]. Paul generates some new potential parameters for CH_4 combustion. Durant and Paul used the program Gaussian-92 in the "Self Consistent Field" mode to compute molecular polarizabilities that are used to estimate dispersion coefficients, well depths, and the location of the potential minimum [49]. The latter is achieved by employing the generalized correlations between van der Waals interaction potential parameters and molecular polarizabilities developed by the Pirani group [50]. The methodology of Tang and Toennies [25] is used to determine the scaling parameters for the exponential repulsive potential using estimated values of ε and R_m, where R_m is the internuclear separation at the potential minimum. By using this methodology, they are able to generate the requisite five potential parameters from three of them. Since many of the species considered are radicals, for which there are few or no measurements, questions about the

accuracy of this approach remain. Other modifications by Paul are concerned with binary thermal diffusion factors and thermal conductivities. They provide a new method for calculating thermal diffusion factors. They adopt the approach of Uribe et al. [51][52] for thermal conductivities, and this enables them to obtain properties for mixtures without using a multicomponent approach. A table of fitting coefficients for (λ_i/λ_i^m) for various molecules where λ_i and λ_i^m are the pure species thermal conductivities of species i as it is, and as if it were a monatomic molecule, respectively, is provided in Paul's report. Paul and Warnatz [2] also modeled a 13 species CO/H_2 flame. Species considered in the flame modeling study are: CO, CO_2, H, H_2, H_2O, H_2O_2, HO_2, O, O_2, OH, and N_2 and they provide new potential parameters for them. Potential parameters for some of the species were taken from MKC, others were obtained by fitting, while the others were obtained from calculated polarizabilities and correlations.

V. 4. Ern and Giovangigli

Calculation of transport properties of mixtures has historically been computationally intensive. In the early 1960s, Monchick, Yun, and Mason (MYM) [53] applied the approach of Wang Chang et al. [54] to derive a nonsymmetric system of equations that can be solved to determine the transport properties. Solving such a system can present a substantial computational cost when the system must be solved many thousands of times, as happens when simulating spatially- and temporally-varying conditions such as flames.

In contrast, in the 1990s, Ern and Giovangigli (EG) used the formalism of Waldmann and Trubenbacher [55] to derive a symmetric system of equations that can be solved rapidly and accurately using iterative methods. The theoretical and computational approaches developed by EG are described in a series of papers [12-18]. The most thorough discourse on their approach is given in a monograph published in 1994 where they describe their iterative methods for solving linear systems arising from kinetic theory to provide transport coefficients of dilute polyatomic gases in multicomponent mixtures.

In both the EG and MYM approaches, a generalized Boltzmann equation is considered and the theoretical approach is that of a first order Enskog expansion. EG indicate that for each transport coefficient various transport linear systems can be considered that correspond to different choices for the polynomial expansions of the species distribution functions. They also demonstrate that these linear systems can be truncated to obtain accurate approximate values of

all the various transport coefficients while still retaining their symmetric form, and they estimate errors of 10^{-3} are achieved with modest computational effort for multicomponent mixtures. In their book, they also present a chapter on numerical experiments in which they introduce some mixture approximations that are somewhat less accurate but more computationally efficient.

A more recent report by Ern and Giovangigli [56], provides a detailed description of EGLIB, which is a general purpose Fortran library for multicomponent mixture transport property evaluation. In this approach, a number of calculations are of order $(N_S)^2$, where N_S is the number of species in the mixture. They use the TRANLIB database and the TRANLIB evaluation of collision integrals in EGLIB with the formalism developed in their earlier studies of transport linear systems.

VI. Determining Potential Parameters from Viscosity Data

Prior to looking at more complex systems like polar molecules and radical species, and mixtures where combination rules are used to infer unlike molecular interactions from like molecular interactions, we digress a bit and examine using viscosity data to obtain potential parameters.

VI. 1. Pure species

Mourits and Rummens [57] review intermolecular potentials based upon viscosity measurements, and discuss the fact that many combinations of the potential parameters, ε_i and σ_i, can be used to calculate viscosities of acceptable precision (2% or less) for species *i*, even for a range of temperatures. Kim and Ross [58] had previously pointed out that at a given temperature, there is a curve in (ε, σ) along which the viscosity is constant, and they determined the shape of the curve for some special cases of reduced temperature for which analytical approximations for the collision integral are available. However, the non-uniqueness or indeterminacy of the potential parameters has not been recognized in many disciplines, including the combustion and chemical physics communities that use transport properties in various applications.

Wang and Law [59] remark that an accurate description of species diffusion is one of the most important elements towards the development of quantitative reaction models of flame

processes. They single out the importance of H atom binary diffusion coefficients $D_{H,i}$, and state that the accuracy of these depends primarily on the accuracy of the L-J potential parameters and the accuracy of the combination rules. Although they did not recognize the non-uniqueness of the potential parameters, they review these parameters derived from a variety of sources, remark on their differences, and note that despite the considerable differences in some of the L-J parameters, differences in their predicted binary diffusion coefficients can be small. They suggest that compensating errors might be responsible for this. Note this is not true for all sets of parameters examined. In a later study, Middha et al. [1] demonstrated that differences in the intermolecular potential parameters produce differences that are significant in the diffusion coefficients; however, these differences are more important at temperatures greater than 1000 K. Paul [49], Paul and Warnatz [2], and Mehdipour and Eslami [60] also did not recognize that the potential parameters are non-unique.

Bastien et al. [61] collected recent viscosity data for a number of substances and temperatures and used Powell's method as described by Press et al. [62] with a brute force fitting approach to determine ε and σ. They found a nearly linear "trough" in ε, σ space, such that any parameter pair in the trough yields a viscosity that agrees with experiment within about 1%, as quantified by the absolute mean relative error

$$\Delta = \frac{1}{N_{\text{exp}}} \sum_{k=1}^{N_{\text{exp}}} \frac{\left| \eta_{calc}^{k} - \eta_{\text{exp}}^{k} \right|}{\eta_{\text{exp}}^{k}} \tag{49}$$

as shown on Figure 2. Although the existence of the trough is closely related to the non-uniqueness of potential parameters as discussed above, in this case the result applies to a range of temperatures rather than a single temperature. One (ε, σ) pair provides the best fit to data, for each of the systems and temperature ranges investigated, but points nearby in the trough fit nearly as well. The trough is found for both pure species and for mixtures. Figure 3 shows the trough for O_2 + SF_6. As indicated by both Figure 2 and Figure 3, the trough is nearly a straight line. The uncertainty in ε is generally on the order of 10% while the uncertainty in σ is less than 3%. The point in (ε, σ) parameter space that leads to the best fit to viscosity data is sensitive to small changes in the data, so different sets of experiments may lead to very different parameter estimates. Therefore, simply quoting the best-fit parameter values does not allow comparison

with the results of other experiments or predictions: the location in parameter space may differ, but the viscosity predictions may be nearly the same. For this reason, Bastien et al. recommend that the slope of the trough be reported along with the best-fit values of σ and ε. If different researchers obtain the same equation for the "trough," then their potential parameters are functionally the same even if they are not identical.

Transport data has frequently been used to acquire information about the intermolecular potential assuming the potential to be of the form $U(r) = \varepsilon\varphi(r/\sigma)$ where φ is the shape function. There are contradictory reports about the efficacy of this in the literature. Many (Brown and Munn [63] and references therein) have indicated that non-equilibrium properties are severe constraints on the intermolecular potential even though the relationship between the non-equilibrium and equilibrium properties and the potential may not be unique. In contrast and more in concert with current results, Kim and Ross [58] and Barker and Pompe [64] indicated that diffusion coefficients are remarkably insensitive to the intermolecular potential. The insensitivity of viscosity to the potential is not widely known in the chemical physics community as well. The non-uniqueness of potential parameters also has not been recognized in recent studies where highly accurate measurements of transport properties are used to constrain the intermolecular potential in a multi-property analysis, e.g., Cappelletti et al. [65]. While transport properties may constrain the potential in a multi-property analysis, they are not a severe constraint as suggested earlier.

Using viscosity measurements as a metric allows the evaluation of the effectiveness of various theoretical approaches in replicating experimental values for various classes of molecules for the range $1 < T^* < 10$. The supporting data associated with the various approaches is used and the molecules and their data are listed in Table 4 and Table 5.

TRANLIB, MKC, and DRFM agree well with experiments for rare gases, and DRFM only differs from MKC for polar molecules. The results for rare gases indicate that the collision integral calculations for MKC, DRFM and TRANLIB yield nearly identical results. Since most combustion occurs in air, the transport properties of nitrogen are important in mixture and multi-component combustion modeling calculations. Figure 4 and Figure 5 and provide the deviation plots for molecular oxygen and nitrogen, respectively. As shown in Figure 4 DRFM does quite well in predicting the molecular oxygen viscosity (deviation of about 0.5 %), while the errors in

the TRANLIB viscosities are larger (about 3 %) and increases with temperature, most likely due to the length and energy scaling parameters, σ and ε. The observations are similar for molecular nitrogen; the error in TRANLIB is smaller (about 0.5 %). Carbon dioxide errors are also small, usually less than 1%. DRFM exhibits relative errors greater than 4% at low temperature for methane (not shown), but these are reduced significantly for temperatures greater than 150 K, while the deviations for TRANLIB are of opposite sign. It would appear that the potential scaling parameters might underlie these deviations, which decrease with temperature.

VI. 2. Polar Molecules

There are not many viscosity measurements for polar molecules, which are required to evaluate the importance of dipole moment corrections. MKC did not consider polar molecules. TRANLIB treats polar molecules by using the Stockmeyer potential, while DRFM scales the length and energy parameters of the potential according to an approach put forth by Hirschfelder et al. [32]. Paul provides scaling factors for ε and σ that are applicable when one or both interacting molecules are polar. These are based on dipole-dipole and dipole-induced-dipole interaction; see Equations (43)-(48). Equations (43) and (44) provide the scaling for ε_i and σ_i, respectively.

Unfortunately there are many polar molecules (e.g., radical species) for which no dipole moment is provided in the TRANLIB parameter set, and even more molecules that are assigned zero polarizability. The lack of dipole moments in particular is a major shortcoming, and correcting it should be a high priority.

TRANLIB does not require the polarizability for the interactions of two polar molecules, but DRFM does. The required molecular data (potential parameters, dipole moments, and polarizability) for both H_2O and NH_3 are tabulated in Table 6.

We performed a series of numerical experiments to assess the importance of the dipole correction. The results are shown in Figure 6 and Figure 7 for H_2O and NH_3, respectively. When we use the TRANLIB program and its supporting data for H_20, we obtain very good agreement with experiment. We assess the magnitude of the effect of polarity by setting the dipole moment of water to zero and comparing its calculated viscosity with viscosity computed with the correct (non-zero) dipole moment. The effect on viscosity is quite large at room temperature (in excess of 80 %), decreases with temperature, and is less than 40% at 450 K. In contrast, if we use the

parameters tabulated for H_20 in DRFM, we find quite large deviations, but it is not obvious whether this is due to incorrect parameters in the DRFM parameter set or to a problem with the DRFM correction for dipoles. As with the TRANLIB numerical experiment discussed above, we set the dipole moment and polarizability of H_2O to zero, and use the DRFM program and potential parameters to calculate the viscosity. Results are close to those obtained for H_20 in TRANLIB with the dipole moment set to zero. That is, TRANLIB and DRFM, used with their respective input potential parameters, predict similar viscosity values for H_20 when the dipole moment and polarizabilities are set to zero. Viscosity calculations with correct values of the dipole moments that are tabulated in Table 6 agree well with experimental values only for TRANLIB. The dipole correction in DRFM is likely to be incorrect.

TRANLIB and its supporting data also predict the NH_3 viscosity with small deviations. The DRFM parameter set does not contain potential parameters for NH_3, so we obtain them by fitting ε_i and σ_i to yield the best fit to data. The values for the dipole moment and polarizability are taken from the Handbook of Chemistry [66]. As before, we assess the importance of the correction for polar molecules in DRFM and TRANLIB by setting the dipole moment and polarizability of NH_3 equal to zero and re-calculating the viscosity as a function of temperature, shown in Figure 7. Deviations are large at low temperature, and decrease with temperature.

Although the available data for polar molecules are limited, we recommend using the TRANLIB approach because it appears to be more reliable, and its scientific foundations are stronger.

VI. 3. Radical Species

There is a dearth of experimentally determined radical species viscosities because they are difficult to measure due to their high reactivity. Cheng and Blackshear [67] measured the viscosity of mixtures of atomic hydrogen and molecular hydrogen, reported results for the pure species (H and H_2) and binary mixtures for the temperature range 200 to 373 K, and compared their results with earlier experiments conducted by Browning and Fox [68]. Cheng and Blackshear viscosities tend to be lower than those of Browning and Fox, and the lack of agreement is attributed to differences in flow regimes. Figure 9 shows how the TRANLIB and DRFM values calculated with their supporting data compare with the measured values. Viscosity 1 is for pure H and its deviations are large, especially for TRANLIB where deviations

larger than 75 % are noted for the higher temperatures; viscosity 2 is H_2 and it has the smallest deviations including Cheng and Blackshear's values. The symbol, 12, represents the H + H_2 interaction viscosity. Its deviations for viscosities calculated by Cheng and Blackshear are quite small; the TRANLIB deviations are smaller than 20 % and often smaller than 10 %, while those associated with DRFM are larger than 30%.

Diffusion coefficients of the radical species, OH, HO_2, and O_3 in He and of OH in air were measured at a single temperature by Ivanov et al. [69], Remorov et al [70], Bertram et al. [71], and Bedjanian et al. [72] and are listed in Table 7. The experimental diffusion coefficients agree well with each other, and with Ivanov et al.'s calculated values. The DRFM OH + He diffusion coefficient is too low compared to experimental values, and the TRANLIB value is too high. Although high, the DRFM values yield better agreement with experiment for HO_2 + He than TRANLIB, and TRANLIB does very well for O_3 + He. To understand the discrepancies, it is important to examine the supporting data, and recall that the transport property sensitivity to σ is about an order of magnitude greater than the sensitivity to ε. Fortunately, the potential parameters used for He are similar in TRANLIB, DRFM, and Ivanov et al. With the exception of He, the different data sets have quite different parameters for each molecule. We calculated the diffusion coefficient for OH + He and HO_2 + He using TRANLIB but with different parameters, and designate these as TRANLIB2. The parameters are: (1) the dipole moments from Ivanov et al., (2) polarizabilities from Paul, and (3) the potential parameters of H_2O as a surrogate for OH and H_2O_2 for HO_2. Ivanov et al. assumed that H_2O is the polar analog of OH and H_2O_2 is the polar analog of HO_2, based on the similarity of their dipole moments. TRANLIB2 parameters are listed in Table 8. Diffusion coefficients for TRANLIB2 are 673.4 and 553.0 cm2 s^{-1} for He with OH and HO_2, respectively. The TRANLIB2 diffusion coefficient of He + OH agree very well with experiment. Deviations of the TRANLIB2 OH and HO_2 diffusion coefficients from the Ivanov et al. measured values are 1.7 and 28.6% as shown in Figure 9.

These comparisons again stress the importance of revisiting the supporting data in TRANLIB. Ivanov et al. showed that calculated diffusion coefficients give better agreement with experimental values if the potential parameters from the polar analogs (H_2O for OH) and (H_2O_2 for HO_2) are used rather than the non-polar analogs O and O_2, respectively. Using this type of approximation might help obtain parameters for radical species for which there are no direct experimental data.

VI. 4. Combining rules:

Mourtis and Rummens point out that finding suitable potential parameters for mixtures is harder than for single species. Combining rules are used to predict the potential parameters characterizing the interactions of two unlike molecules from parameters characterizing each of the individual molecules. There has long been debate about the suitability of different combination rules [see for example, Maitland et al. [20], Bzowski et al. [10], and Paul [49]]. The most commonly used combining rule for the collision diameter is the arithmetic mean (AM):

$$\sigma_{ij} = \frac{\sigma_{ii} + \sigma_{jj}}{2} \tag{50}$$

This rule is exact under the assumption that the interacting molecules are hard spheres. The most commonly used combining rule for the well depth is the geometric mean (GM), also called the Berthelot rule:

$$\varepsilon_{ij} = \sqrt{\varepsilon_{ii}\varepsilon_{jj}} \tag{51}$$

In practice, this rule often overestimates the strength of the interactions between unlike molecules, and in response to this, other rules have been proposed which give more weight to the component with the weaker intermolecular forces [20]. One of these is the harmonic mean (HM), originally advocated by Fender and Halsey (1962) [73]:

$$\varepsilon_{ij} = \frac{2\varepsilon_{ii}\varepsilon_{jj}}{\varepsilon_{ii} + \varepsilon_{jj}} \tag{52}$$

More sophisticated combining rules like that of Kong [74] (KR) have been proposed for σ_{ij} and ε_{ij}:

$$\sigma_{ij} = \frac{\left[\left(\varepsilon_{ii}\sigma_{ii}^{12}\right)^{1/13} + \left(\varepsilon_{jj}\sigma_{jj}^{12}\right)^{1/13}\right]^{13/6}}{2^{13/6}\left(\varepsilon_{ii}\varepsilon_{jj}\right)^{1/12}\left(\sigma_{ii}\sigma_{jj}\right)^{1/2}} \tag{53}$$

$$\varepsilon_{ij} = \frac{\varepsilon_{ii}\varepsilon_{jj}\sigma_{ii}^{6}\sigma_{jj}^{6}}{\left(\varepsilon_{ii}\sigma_{ii}^{12}\right)/2^{13} \cdot \left\{1 + \left[\left(\varepsilon_{jj}\sigma_{jj}^{12}\right)/\left(\varepsilon_{ii}\sigma_{ii}^{12}\right)\right]^{1/13}\right\}^{13}} \tag{54}$$

As discussed above, Bastien et al. [61] demonstrated that the parameters for individual pure species and binary mixtures are not uniquely determined by a set of viscosity measurements: the

(ε_{ij}, σ_{ij}) values that fit a set of experimental data with low uncertainty define a nearly linear "trough" in parameter space. A single point provides the best viscosity predictions, but values elsewhere on the trough provide reasonable predictions. They also found that the various combining rules presented above for a given mixture yields quite different values for pairs of potential parameter. It is often stated that all of the combining rules tend to under-predict the viscosity; Bastien et al. found this not to be strictly the case. Relative to combined parameters that they found from fitting transport properties for binary mixtures, the arithmetic mean overpredicts the collision diameter. Kong's rule overestimates it even more. Kong's rule, however, underestimates the combined ε_{ij}, thus yielding a (ε, σ) pair on or near the trough and leading reasonably good viscosity predictions in most cases. They observed no consistent over- or under-prediction in the viscosity when the geometric mean or the harmonic mean rules are used.

VII. Transport Properties for T* >10.0

Mason, Kestin, and their various colleagues observed a slight failure in the Law of Corresponding States when the LJ 12-6 potential was used for values of T* greater that 10 and suggested that for high T* it should be replaced by a Born-Mayer exponential repulsive potential, $U(r)=U_o\exp(-r/\rho)$, thereby introducing two additional parameters.

The Born-Mayer potential parameters can be evaluated using a damping function approach as suggested by Tang and Toennies [25] when R_m, ε, and the dispersion constants (mostly C_6) are known. Pirani and colleagues (Pirani et al. [75] and Cambi et al. [50]) suggest an approach to finding the L-J potential parameters that is based on molecular polarizability. If the correlations they determine are used, R_m (the distance of the minimum of potential), ε, and the dispersion parameters can be estimated. These empirical relationships can be used to generate the set of potential parameters required for transport property calculations over a broad range of temperatures. Each parameter is a potential source of error, and as the number of parameters increases, the errors can multiply, and potentially cause some serious errors in modeling studies.

It is of interest to evaluate if there are benefits acquired by using the Born-Mayer potential even if there is the possibility of additional parameter errors. Unfortunately data spanning the temperature range of interest is only available for a few molecules. We found data for the molecules Ne, H_2, and N_2. Figure 10 is a deviation plot for Ne where the viscosity is calculated two ways: using the LJ 12-6 potential over the entire T* range or replacing it with the Born Mayer potential at the T* greater than 10. The two approaches track one another and give nearly identical answers. The same is true for H_2 and N_2 as shown in Figure 11 and Figure 12, respectively. In fact, for N_2, we observe that the predictions are better when using a pure L-J potential. It is interesting that in the case of N_2, the Born Mayer potential does not work for T* less than 10, while for the other molecules, it would be acceptable.

At this time, based on the very limited data that we have, we would recommend using the L-J potential over the entire temperature range since using it offers the possibility of fewer errors since fewer parameters are required. We also recommend that the benefits and limitations of using the LJ potential for T* greater that 10 continue to be evaluated as more data become available.

VIII. Thermal Conductivity

Thermal conductivity for monatomic gases is computed with the same collision integral as used for viscosity: $\Omega^{(2,2)*}$, and it requires similar potential parameters for evaluation. With the exception of monatomic species, it is actually more complex because of the importance of inelastic collisions. We have made a limited study of thermal conductivity for a few non-polar molecules and one binary mixture by comparing calculated values of thermal conductivity with experimental values.

The various treatments of energy transfer to support calculations of thermal conductivity vary among TRANLIB, DRFM, MKC, and EGLIB. Each approaches shares a common guiding principle, namely, that one can evaluate contributions of the various degrees of freedom separately, and that the thermal conductivity is the sum of the contribution from the various internal degrees of freedom. This is the so-called Wang Chang-Uhlenbeck-de Boer (WCUB) [54] theory that has been used and modified slightly by many others.

The contribution of the translational degrees of freedom is evaluated by assuming that the molecule of interest is monatomic and by using formulae appropriate for rare gases. The evaluation of the contributions of the internal degrees of freedom is handled differently by the four approaches. The flow of energy to the various internal degrees of freedom is often assumed to occur by a diffusion process and the diffusion coefficients associated with the various degrees of freedom are approximated differently. MKC assumes that there are different diffusion coefficients associated with each of the degrees of freedom, and TRANLIB uses the same diffusion coefficient for pure species thermal conductivities that they use for mixture averaged thermal conductivities for all the degrees of freedom. Yet for the limited number of molecules whose thermal conductivity we have evaluated, they produce quite similar results. TRANLIB, MKC, and DRFM only provide for the calculation of mixture averaged properties for thermal conductivity. EGLIB is the only code that provides a multicomponent treatment for thermal conductivity.

As one might expect, the most important energy transfer processes are those involving the translational and rotational degrees of freedom. This is why the rotational relaxation collision number is important in most formalisms. Theories for its temperature dependence have been presented by Brau and Jonkman [76] and Parker [77], but only for homonuclear diatomic molecules. The collision number for rotational relaxation can be measured by a number of techniques like sound absorption and even thermal conductivity measurements. Internal rotations, which are important at thermal energies, have not been treated in any of the approaches. These are important especially for more complex fuel molecules. As molecules become more complex and temperature increases as it does in combustion, other degrees of freedom will become important. Thermal conductivities of strongly polar gases are anomalously low, and we expect this to be the case for the thermal conductivities of radical species.

Thermal conductivity, unlike other transport properties, depends on thermo-chemistry. A quantity that is often used for estimating the effects of energy transfer on thermal conductivity is the heat capacity. Frequently, the contribution of the internal degrees of freedom to the thermal conductivity has been estimated by using a Eucken correction. The coefficient of thermal conductivity for a polyatomic gas is estimated to be the product of the thermal conductivity coefficient, assuming that the gas is monatomic, times the Eucken factor

$$\frac{\lambda}{\lambda_{mon}} = \frac{4}{15}\frac{C_v}{R} + \frac{3}{5} \qquad (55)$$

where C_v is the heat capacity at constant volume. Hirschfelder derived an improved Eucken factor, 0.354 (C_v/R) + 0.469. Frequently the Eucken factor approach has been over-valued and many think that thermal conductivity is a solved problem. This is not the case. Hirschfelder indicated that the Eucken factor does not seem to be applicable to the rotational degrees of freedom for polar gases near room temperature, Mason and Monchick [78] indicated that the Eucken factors can vary considerably for different molecules.

IX. Summary and Conclusions

This review examines current approximations and approaches that underlie the evaluation of transport properties for combustion modeling applications. Discussed in the review are: the intermolecular potential and its descriptive molecular parameters; various approaches to evaluating collision integrals; supporting data required for the evaluation of transport properties; the quality of experimental measurements and their importance for validating or rejecting approximations to property estimation; the interpretation of corresponding states; combination rules that yield pair molecular potential parameters for unlike species from like species parameters; and mixture approximations. The insensitivity of transport properties to intermolecular forces is noted, especially the non-uniqueness of the supporting potential parameters. Viscosity experiments of pure substances and binary mixtures measured post 1970 are used to benchmark a number of approximations, and the intermediate temperature range $1 < T^* < 10$, where T^* is kT/ε, is emphasized since this is where rich data sets are available. When suitable potential parameters are used, the accuracy of transport property evaluation for pure substances and binary mixtures is acceptable when they are calculated using the approaches of Kee et al. [6], Mason, Kestin, and Uribe [7-11], Paul and Warnatz [2], Ern and Giovangigli. [12-18]. Although the approach to treating polar molecules appears to be different in TRANLIB and DRFM, they yield quite similar results when the supporting data required by each is accurate. Recommendations from the review include a strong plea for revisiting the supporting data required by the various approaches, and updating the data sets with accurate potential parameters, dipole moments, and polarizabilities. Potential parameters and the slope of the trough line should be reported for the molecules in the supporting data sets. We also recommend

using the TRANLIB approach for treating polar molecules. Combining rules were found to under predict the viscosity in most of the cases, and Kong's rule was found to work better than the others, but we recommend that improved rules be developed. There are very few measurements of transport properties for radical species, and enter a strong recommendation for additional measurements. Thermal conductivity, which is important for the fuel and oxidizer in the early stages of flame development, must have accurate values of the molecular heat capacity for its evaluation.

References

[1] Middha P, Yang BH, Wang H. A First-Principle Calculation of the Binary Diffusion Coefficients Pertinent to Kinetic Modeling of Hydrogn-Oxygen-Helium Flames. Proc Combust Inst 2002;29:1361-9.

[2] Paul PH, Warnatz J. A Re-Evaluation of the Means Used to Calculate Transport Properties of Reacting Flows. Proc Combust Inst 1998;27:495-504.

[3] Grcar JF, Bell JB, Day MS. The Soret Effect in Naturally Propagating, Premixed, Lean, Hydrogen-Air Flames. Proc Combust Inst 2009;32:1173-80.

[4] Brown NJ, Revzan KL. Comparative Sensitivity Analysis of Transport Properties and Reaction Rate Coefficients. Int J Chem Kinet 2005;37:538-53.

[5] Wakeham WA, Assael MA, Atkinson JK, Bilek J, Fareleira JMNA, Fitt AD, Goodwin ARH. Thermophysical Property Measurements: The Journey from Accuracy to Fitness for Purpose. Int J Thermophys 2007;28:372-416.

[6] Kee RJ, Dixon-Lewis G, Warnatz J, Coltrin ME, Miller JA. A FORTRAN Computer Code Package for the Evaluation of Gas-Phase Multicomponent Transport Properties. SANDIA; 1986.

[7] Najafi B, Mason EA, Kestin J. Improved Corresponding States Principle for the Noble Gases. Physica A 1983;119:387-440.

[8] Kestin J, Knierim K, Mason EA, Najafi B, Ro ST, Waldman M. Equilibrium and Transport Properties of the Noble Gases and their Mixtures at Low Density. J Phys Chem Ref Data 1984;13:229-303.

[9] Boushehri A, Bzowski J, Kestin J, Mason EA. Equilibrium and Transport Properties of Eleven Polyatomic Gases at Low Density. J Phys Chem Ref Data 1987;16:445-66.

[10] Bzowski J, Kestin J, Mason EA, Uribe FJ. Equilibrium and Transport Properties of Gas Mixtures at Low Density: Eleven Polyatomic Gases and Five Noble Gases. J Phys Chem Ref Data 1990;19:1179-232.

[11] Mason EA, Uribe FJ. The Corresponding-States Principle - Dilute Gases. In: Millat J, Dymond JH, Nieto de Castro CA, editors. Transport Properties of Fluids : Their Correlation, Prediction, and Estimation. 1st Ed, Cambridge: Cambridge University Press; 1996, p. 250-282.

[12] Ern A, Giovangigli V. Multicomponent Transport Algorithms. Heidelberg: Springer-Verlag; 1994.

[13] Ern A, Giovangigli V. Thermal Conduction and Thermal Diffusion in Dilute Polyatomic Gas Mixtures. Physica A 1995;214:526-46.

[14] Ern A, Giovangigli V. Fast and Accurate Multicomponent Transport Porperty Evaluation. J Comput Phys 1995;120:105-16.

[15] Ern A, Giovangigli V. On the Evaluation of Thermal Diffusion Coefficients in Chemical Vapor Deposition Processes. Chem Vapor Depos 1995;3:3-31.

[16] Ern A, Giovangigli V. Volume Viscosity of Dilute Polyatomic Gas Mixtures. Eur J Mech B-Fluids 1995;14:653-69.

[17] Ern A, Giovangigli V. The Structure of Transport Linear Systems in Dilute Isotropic Gas Mixtures. Phys Rev E 1996;53:485-92.

[18] Ern A, Giovangigli V. Projected Iterative Algorithms with Application to Multicomponent Transport. Linear Algebra Appl 1997;250:289-315.

[19] Lemmon EW, Huber ML, McLinden MO. NIST Reference Fluid Thermodynamic and Transport Properties - REFPROP 8.0. US Department of Commerce, National Institute of Standards and Technology; 2008.

[20] Maitland GC, Rigby M, Smith EB, Wakeham WA. Intermolecular forces: their origin and determination. Oxford: Clarendon Press; 1981.
[21] Drude PKL. The Theory of Optics. London: Longman; 1933.
[22] Stallcop JR, Partridge H, Walch SP, Levin E. H-N2 Interaction Energies, Transport Cross Sections, and Collision Integrals. J Chem Phys 1992;97:3431-6.
[23] Partridge H, Bauschlicher Jr CW, Stallcop JR, Levin E. Ab Initio Potential Energy Surface for H-H2. J Chem Phys 1993;99:5951-60.
[24] Stallcop JR, Partridge H, Levin E. H-H2 Collision Integrals and Transport Coefficients. Chem Phys Lett 1996;254:25-31.
[25] Tang KT, Toennies JP. An Improved Simple Model for the Van Der Waals Potential Based on Universal Damping Functions for the Dispersion Coefficients. J Chem Phys 1984;80:3726-41.
[26] Stallcop JR, Partridge H, Levin E. Ab Initio Potential-Energy Surfaces and Electron-Spin-Exchange Cross Sections for H-O2 Interactions. Phys Rev A 1996;53:766-71.
[27] Stallcop JR, Levin E, Partridge H. Transport Properties of Hydrogen. J Thermophys Heat Transfer 1998;12:514-19.
[28] Stallcop JR, Partridge H. The N2-N2 Potential Energy Surface. Chem Phys Lett 1997;281:212-20.
[29] Stallcop JR, Partridge H, Levin E. Effective Potential Energies and Transport Cross Sections for Interactions of Hydrogen and Nitrogen. Phys Rev A 2000;62:062709.
[30] Stallcop JR, Partridge H, Pradhan A, Levin E. Potential Energies and Collision Integrals for Interactions of Carbon and Nitrogen Atoms. J Thermophys Heat Transfer 2000;14:480-88.
[31] Stallcop JR, Partridge H, Levin E. Effective Potential Energies and Transport Cross Sections for Atom-Molecule Interactions of Nitrogen and Nitrogen. Nasa: Ames Research Center; 2001.
[32] Hirschfelder JO, Curtiss CF, Bird RB. Molecular Theory of Gases and Liquids. New York: John Wiley and Sons, Inc.; 1954.
[33] Kestin J, Wakeham WA. Transport Properties of Fluids - Thermal Conductivity, Viscosity, and Diffusion Coefficient. New York: Hemisphere Publishing Corporation; 1988.
[34] Kestin J, Khalifa HE, Ro ST, Wakeham WA. Viscosity and Diffusion Coefficients of Eighteen Binary Gaseous Systems. Physica A 1977;88:242-60.
[35] Retsina T, Richardson SM, Wakeham WA. The Theory of a Vibrating-Rod Viscometer. Appl Sci Res 1987;43:325-46.
[36] Seibt D, Vogel E, Bich E, Buttig D, Hassel E. Viscosity Measurements on Nitrogen. J Chem Eng Data 2006;51:526-33.
[37] Langelandsvik LI, Solvang S, Rousselet M, Metaxa IN, Assael MJ. Dynamic Viscosity Measurements of Three Natural Gas Mixtures - Comparison against Prediction Models. Int J Thermophys 2007;28:1120-30.
[38] Haarman JW. Ph.D. Thesis. Netherlands: Technische Hogeschool Delft; 1969.
[39] Kee RJ, Warnatz J, Miller JA. A FORTRAN Computer Package for the Evaluation of Gas-Phase Viscosities, Conductivities, and Diffusion Coefficients. SANDIA; 1983.
[40] Monchick L, Mason EA. Transport Properties of Polar Gases. J Chem Phys 1961;35:1676-97.
[41] Wilke CR. A Viscosity Equation for Gas Mixtures. J Chem Phys 1950;18:517-19.
[42] Bird RB, Stewart WE, Lightfoot EN. Transport Phenomena. New York: John Wiley and Sons; 1960.
[43] Grcar JF. The Chemkin Transport Package. Lawrence Berkeley National Laboratory; 1999.
[44] Parson JM, Schafer TP, Tully FP, Siska PE, Wong YC, Lee YT. Intermolecular Potentials from Crossed Beam Differential Elastic Scattering Measurements. I. Ne+Ar, Ne+Kr, and Ne+Xe. J

Chem Phys 1970;53:2123.
[45] Parson JM, Schafer TP, Siska PE, Tully FP, Wong YC, Lee YT. Intermolecular Potentials from Crossed Beam Differential Elastic Scattering Measurements. II. Ar+Kr and Ar+Xe. J Chem Phys 1970;53:3755.
[46] Scoles G. Two-Body, Spherical, Atom-Atom, and Atom-Molecule Interaction Energies. In: Annual Review of Physical Chemistry, Palo Alto, CA: Annual Reviews Inc.; 1980, p. 81-96.
[47] McCourt FRW, Terhorst MA, Jameson CJ. N2-Kr Interaction - A Multiproperty Analysis. J Chem Phys 1995;102:5752-60.
[48] McCourt FRW, Terhorst MA, Heck EL, Dickinson AS. Transport Properties of He-CO Mixtures. Mol Phys 2002;100:3893-906.
[49] Paul PH. DRFM, A New Package for the Evaluation of Gas-Phase-Transport Properties. SANDIA National Laboratories: SAND98-8203 UC-1409; 1997.
[50] Cambi R, Andre RP, Cappelleti D, Liuti G, Pirani F. Generalized Correlations in Terms of Polarizability for Van Der Waals Interaction Potential Parameter Calculations. J Chem Phys 1991;95:1852-61.
[51] Uribe FJ, Mason EA, Kestin J. A Correlation Scheme For The Thermal Conductivity of Polyatomic Gases at Low Density. Physica A 1989;156:467-91.
[52] Uribe FJ, Mason EA, Kestin J. Thermal Conductivity of Nine Polyatomic Gases at Low Density. J Phys Chem Ref Data 1990;19:1123-36.
[53] Monchick L, Yun KS, Mason EA. Formal Kinetic Theory of Transport Phenomena in Polyatomic Gas Mixtures. J Chem Phys 1963;39:654-69.
[54] Wang Chang CS, Uhlenbeck GE, de Boer J. Studies in Statistical Mechanics. Amsterdam: North-Holland; 1964.
[55] Waldmann L, Trubenbacher E. Formale Kinetsche Theorie von Gasgemischen aus Anregbaren Molekulen. 1962;A17:363.
[56] Ern A, Giovangigli V. Kinetic theory of Reactive Gas Mixtures with Application to Combustion. Transport Theor Stat 2003;32:657-77.
[57] Mourits FM, Rummens FHA. A Critical Evaluation of Lennard-Jones and Stockmayer Potential Parameters and of Some Correlation Methods. Can J Chem 1977;15:3007-20.
[58] Kim SK, Ross J. On Determination of Potential Parameters from Transport Coefficients. J Chem Phys 1967;46:818.
[59] Wang H, Law CK. Diffusion Coefficient of Hydrogen Atom for Combustion Modeling. Hilton Head, SC: Technical Meeting of the Eastern States Section of the Combustion Institute; 1996.
[60] Mehdipour N, Eslami H. Calculation of Transport Properties of Simple Dense Fluids. Int J Therm Sci 2002;41:949-54.
[61] Bastien LAJ, Price PN, Brown NJ. Intermolecular potential parameters and combining rules determined from viscosity data. Submitted for Publication 2010;.
[62] Press WH, Teukolsky SA, Vetterling WT, Flannery BP. Numerical Recipes in Fortran. Second Edition. New York: Cambridge University Press; 1992.
[63] Brown NJ, Munn RJ. Inert Gas Potentials for Mixed Interactions. J Chem Phys 1972;57:2216-8.
[64] Barker JA, Pompe A. Atomic Interactions in Argon. Aust J Chem 1968;21:1683-94.
[65] Cappelleti D, Vecchiocattivi F, Pirani F, Heck EL, Dickinson AS. An Intermolecular Potential for Nitrogen from a Multi-Property Analysis. Mol Phys 1996;93:485-99.
[66] Lide DR. Handbook of Chemistry and Physics. 84th ed. CRC Press; 2003.
[67] Cheng DY, Blackshear Jr. PL. Measurements on the Viscosity of the Atomic Hydrogen. J Chem Phys 1972;56:213-23.

[68] Browning R, Fox JW. The Coefficient of Viscosity of Atomic Hydrogen and the Coefficient of Mutual Diffusion for Atomic and Molecular Hydrogen. Proc Roy Soc London, Ser A 1964;278:274.
[69] Ivanov AV, Trakhtenberg S, Bertram AK, Gershenzon YM, Molina MJ. OH, HO2, and Ozone Gaseous Diffusion Coefficients. J Phys Chem A 2007;111:1632-7.
[70] Remorov RG, Grigorieva VM, Ivanov AV, Sawerysyn J, Gershenzon YM. 13th Int. Symp. Gas Kinetics. Dublin, Ireland; 1996.
[71] Bertram AK, Ivanov AV, Hunter M, Molina LT, Molina MJ. The Reaction Probability of OH on Organic Surfaces of Tropospheric Interest. J Phys Chem A 2001;105:9415-21.
[72] Bedjanian Y, Lelievre S, Le Bras G. Experimental Study of the Interaction of HO2 Radicals with Soot Surface. Phys Chem Chem Phys 2004;7:334-41.
[73] Fender BEF, Halsey, Jr. GD. Second Virial Coefficients of Argon, Krypton, and Argon-Krypton Mixtures at Low Temperatures. J Chem Phys 1962;36:1881-8.
[74] Kong CL. Atomic Distortion and the Repulsive Interactions of the Noble Gas Atoms. J Chem Phys 1973;59:968-9.
[75] Pirani F, Brizi S, Roncaratti LF, Casavecchia P, Cappelleti D, Vecchiocattivi F. Beyond the Lennard-Jones model: a simple and accurate potential function probed by high resolution scattering data useful for molecular dynamics simulations. Phys Chem Chem Phys 2008;10:5489-503.
[76] Brau CA, Jonkman RM. Classical Theory of Rotational Relaxation in Diatomic Gases. J Chem Phys 1970;52:477-84.
[77] Parker JG. Rotational and Vibrational Relaxation in Diatomic Gases. Phys Fluids 1959;2:449-62.
[78] Mason EA, Monchick L. Heat Conductivity of Polyatomic Polar Gases. J Chem Phys 1962;36:1622-39.
[79] Helleman JM, Kestin J, Ro ST. Viscosity of Oxygen and of some of its Mixtures with other Gases. Physica 1973;65:362-75.
[80] Helleman JM, Ro ST, Kestin J. Viscosity of Binary Gaseous Mixtures of Nitrogen with Argon and Krypton. J Chem Phys 1972;57:4038-42.
[81] Kestin J, Ro ST, Wakeham WA. Viscosity of the Binary Gaseous Mixtures He-Ne and Ne-N2 in the Temperature Range 25-700 °C. J Chem Phys 1972;56:5837-42.
[82] Kestin J, Ro ST, Wakeham WA. Viscosity of the Binary Gaseous Mixture Helium-Nitrogen. J Chem Phys 1972;56:4036-42.
[83] Fokin LR, Kalashnikov AN. The viscosity and self-diffusion of rarefied steam: Refinement of reference data. High Temp 2008;46:614-9.
[84] Burch LG, Raw JG. Transport Properties of Polar-Gas Mixtures - I - Viscosities of Ammonia-Methylamine Mixtures. J Chem Phys 1967;47:2798-801.
[85] Dawe RA, Smith EB. Viscosities of the Inert Gases at High Temperatures. J Chem Phys 1970;52:693-703.
[86] Kestin J, Ro ST, Wakeham WA. Viscosity of the Binary Gaseous Mixture Neon-Krypton. J Chem Phys 1972;56:4086-91.
[87] Kestin J, Ro ST, Wakeham WA. Viscosity of the Noble Gases in the Temperature Range 25 -700 °C. J Chem Phys 1972;56:4119-24.
[88] May EF, Berg RF, Moldover MR. Reference viscosities of H2, CH4, Ar, and Xe at low densities. Int J Thermophys 2007;28:1085-110.
[89] Kestin J, Ro ST, Wakeham WA. Reference Values of the Viscosity of Twelve Gases at 25 °C. Trans Faraday Soc 1971;67:2308-13.

Tables

Table 1: Coefficient of the low-temperature formulas for $\Omega^{(2.2)*}$ and $\Omega^{(1.1)*}$ for noble gases (Kestin et al. [8]).

i	a_{i1}	a_{i2}	b_{i1}	b_{i2}
1	0.18	0	0	0
2	0	0	0	0
3	-1.20407	-0.195866	10.0161	-10.5395
4	-9.86374	20.2221	-40.0394	46.0048
5	16.6295	-31.3613	44.3202	-53.0817
6	-6.73805	12.6611	-15.2912	18.8125

Table 2: Coefficient of the formulas for $\Omega^{(2.2)^*}$ and $\Omega^{(1.1)^*}$ for the range of temperature $1 \leq T^* \leq 10$ (Kestin et al. [8]).

i	a_i (noble and polyatomic gases)	b_i (noble gases)	b_i (polyatomic gases)
0	0.46641	0.357588	0.295402
1	-0.56991	-0.472513	-0.510069
2	0.19591	0.0700902	0.189395
3	-0.03879	0.016574	-0.045427
4	0.00259	-0.00592022	0.0037928

Table 3: Coefficient of the formulas for $\Omega^{(2.2)^*}$ and $\Omega^{(1.1)^*}$ for high temperatures $T^* \geq 10$ (Kestin et al. [8]).

i	a_{i1}	a_{i2}	a_{i3}	a_{i4}	
1	-33.0838	20.0862	72.1052	8.27648	
2	101.571	56.4472	286.393	17.7610	
3	-87.7036	46.3130	277.146	19.0573	
i	b_{i1}	b_{i2}	b_{i3}	b_{i4}	c_i
2	-267.00	201.570	174.672	7.36916	1
4	26700	-19.2265	-27.6938	-3.2955	10^3
6	-8.9×10^5	6.31013	10.2266	2.33033	10^5

Table 4: Scaling potential parameters of some species from TRANLIB and DRFM.

	ε (K)		σ (Å)	
	TRANLIB	DRFM	TRANLIB	DRFM
Ar	136.500	143.20	3.330	3.350
O_2	107.400	121.1	3.458	3.407
N_2	97.530	98.4	3.621	3.652
CO_2	244.000	245.3	3.763	3.769
CH_4	141.400	161.4	3.746	3.721
H_2O	572.400	535.21	2.605	2.673
NH_3	481.000	282.2[1]	2.290	3.30[1]
HO_2	107.400	365.56	3.458	3.433
OH	80.000	281.27	2.750	3.111
H_2O_2	107.400	368.11	3.458	3.499

[1] Fitted values

Table 5: Dipole moment μ and polarizability α of some species from TRANLIB and DRFM.

	μ (Debye)		α (Å^3)	
	TRANLIB	DRFM	TRANLIB	DRFM
Ar	0.000	0	0.000	1.642
O_2	0.000	0	1.600	1.600
N_2	0.000	0	4.000	1.750
CO_2	0.000	0	2.650	2.65
CH_4	0.000	0	2.600	2.60
H_2O	1.844	1.847	0.000	1.450
NH_3	1.470	1.4718[2]	0.000	2.81[2]
HO_2	0.000	2.09	0.000	1.950
OH	0.000	1.655	0.000	0.980
H_2O_2	0.000	1.573	0.000	2.230

[2] Value taken from reference [66]

Table 6: Potential parameters for H_2O and NH_3 in TRANLIB and DRFM with and without the polar correction.

(ε: well depth; σ: collision diameter; μ: dipole moment; α: polarizability)

		ε (K)	σ (Å)	μ (Debye)	α (Å^3)
H_2O	TRANLIB	572.4	2.61	1.844	0
	TRANLIB, without polar correction	572.4	2.61	0	0
	DRFM	535.2	2.67	1.847	1.45
	DRFM, without polar correction	535.2	2.67	0	0
NH_3	TRANLIB	481.0	2.92	1.47	0
	TRANLIB, without polar correction	481.0	2.92	0	0
	DRFM	282.2[3]	3.30[3]	1.4718[4]	0.281[4]
	DRFM, without polar correction	282.2	3.30	0	0

[3] Fitted value
[4] Value taken from reference [66]

Table 7: Binary diffusion coefficients ($cm^2\ s^{-1}$) for the interaction of He with three other radical species measured and computed in different ways.

	OH and He	HO_2 and He	O_3 and He
TRANLIB	673.4	553.0	424.2
DRFM	636.7	526.9	X
Measured by Ivanov et al (2007)	662 ± 33	430 ± 30	410 ± 25
Computed by Ivanov et al (2007)	636.7	407.3	425.4
From Remorov et al. (1996)	609 ± 250	X	X
From Bertram et al. (2001)	665 ± 35	X	X
From Bedjanian et al. (2004)	X	405 ± 50	X
TRANLIB2	666.3	552.6	X

Table 8: Potential constants for OH, He, HO_2, and O_3 from different sources.

		ε (K)	σ (Å)	α (Å^3)	μ (Debye)
OH	TRANLIB	80.000	2.750	0.000	0.000
	TRANLIB2	572.40	2.605	0.98	1.74
	DRFM	281.27	3.111	0.980	1.655
	Ivanov et al (2007)	809.1	2.641	X	1.74
He	TRANLIB	10.200	2.576	0.000	0.000
	TRANLIB2	10.200	2.576	0.200	0.000
	DRFM	10.40	2.610	0.200	0
	Ivanov et al (2007)	10.22	2.556	X	0
HO_2	TRANLIB	107.400	3.458	0.000	0.000
	TRANLIB2	107.400	3.458	1.95	2.090
	DRFM	356.56	3.433	1.950	2.09
	Ivanov et al (2007)	298.3	4.196	X	2.090
O_3	TRANLIB	180.000	4.100	0.000	0.000
	DRFM	X	X	X	X
	Ivanov et al (2007)	106.7	3.467	X	0

Figures

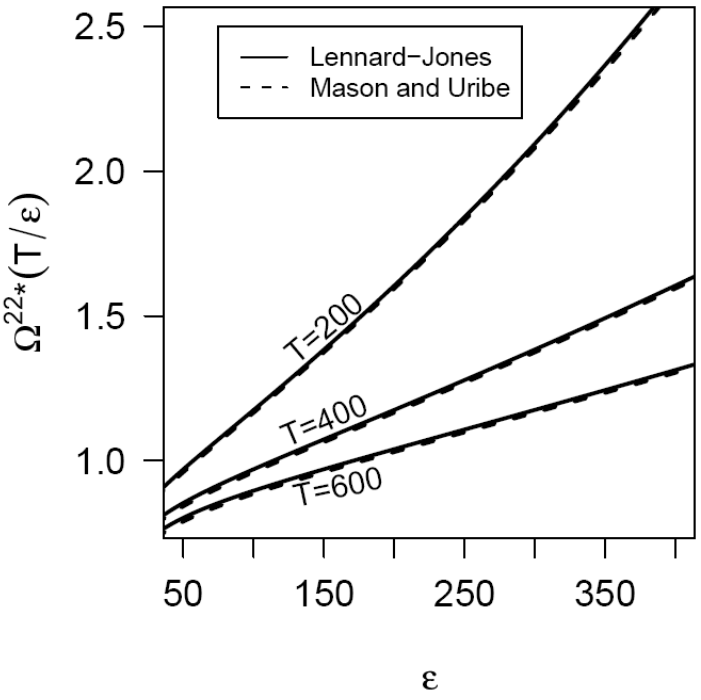

Figure 1: $\Omega^{(2,2)*}$ versus ε for T=200, 400, and 600 K. Values resulting from the empirical fit of Mason and Uribe are very close to those resulting from a Lennard-Jones potential. The curves are nearly linear over a wide range of ε.

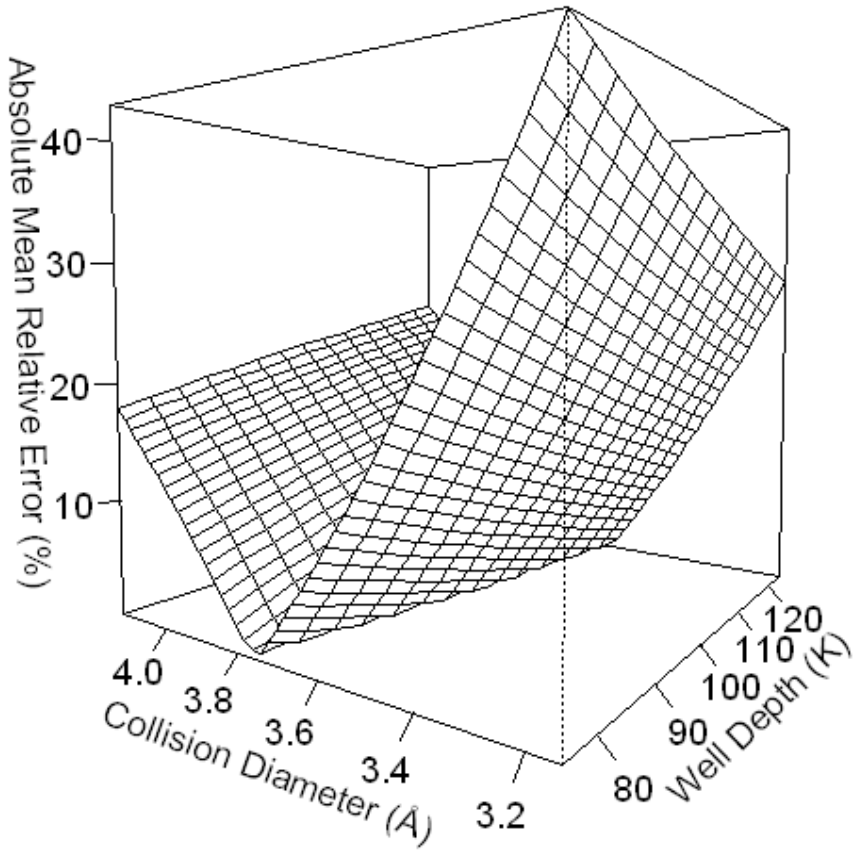

Figure 2: Absolute Relative Mean Error Δ versus the potential parameters ε (well depth) and σ (collision diameter) for the interaction of N_2 with N_2.

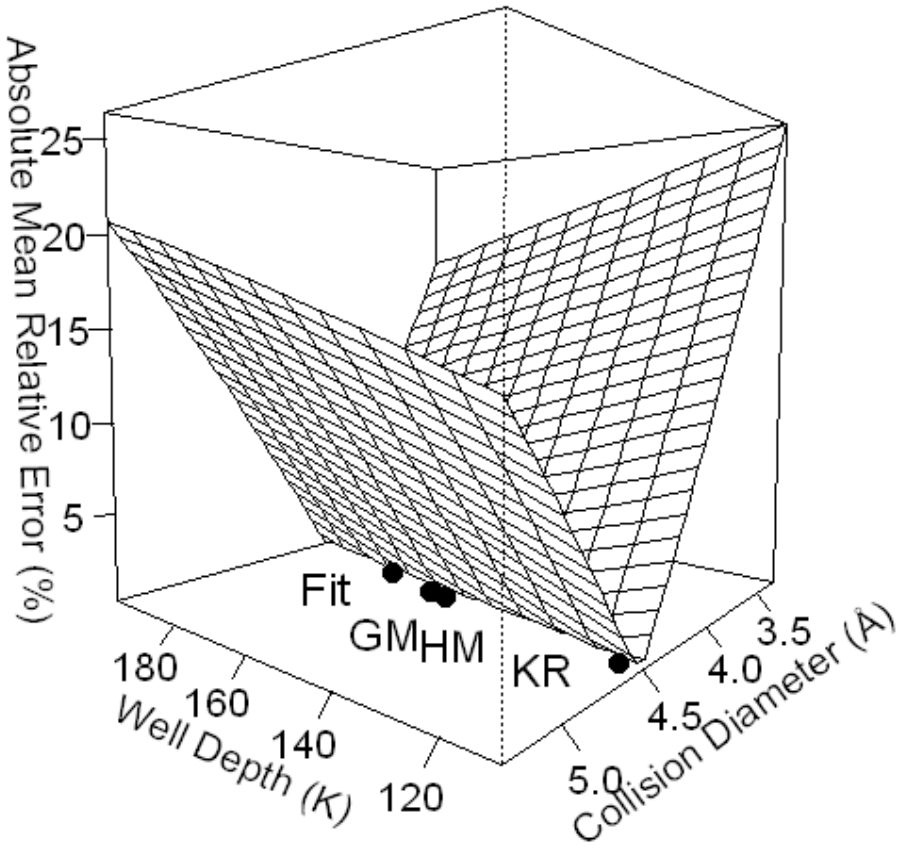

Figure 3: Absolute Relative Mean Error Δ versus the potential parameters ε (well depth) and σ (collision diameter) for the interaction of O_2 with SF_6.

Fit: potential parameter couples obtained by fitting to experiment. GM: ε obtained with the geometric rule and σ obtained with the arithmetic rule. HM: ε obtained with the harmonic mean and σ obtained with the arithmetic mean. KR: ε and σ obtained with Kong's rules.

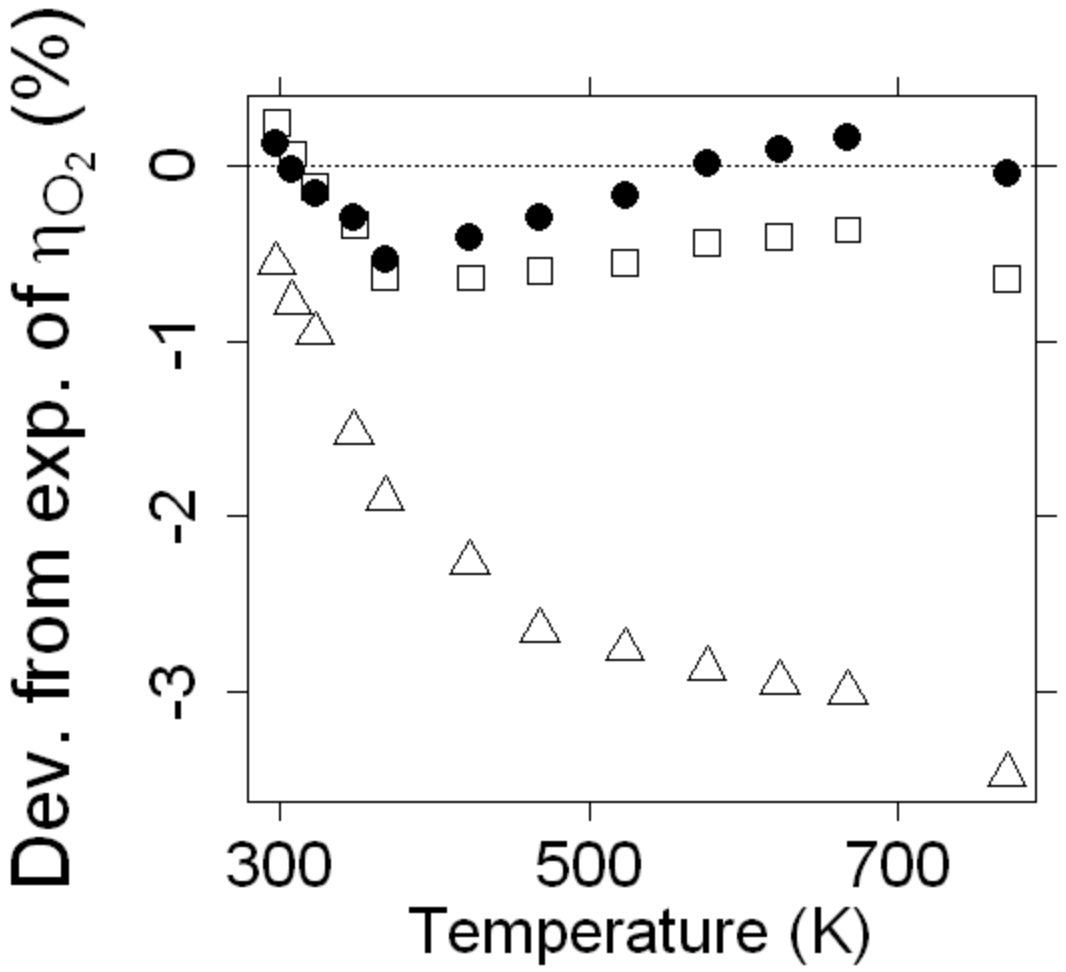

Figure 4: Deviation plot for differences between predicted and experimental viscosity of O_2.

□: MKC/DRFM and △: TRANLIB. ●: MKC/DRFM with fitted parameters from Bastien et al. [61]. Experiments are from [79].

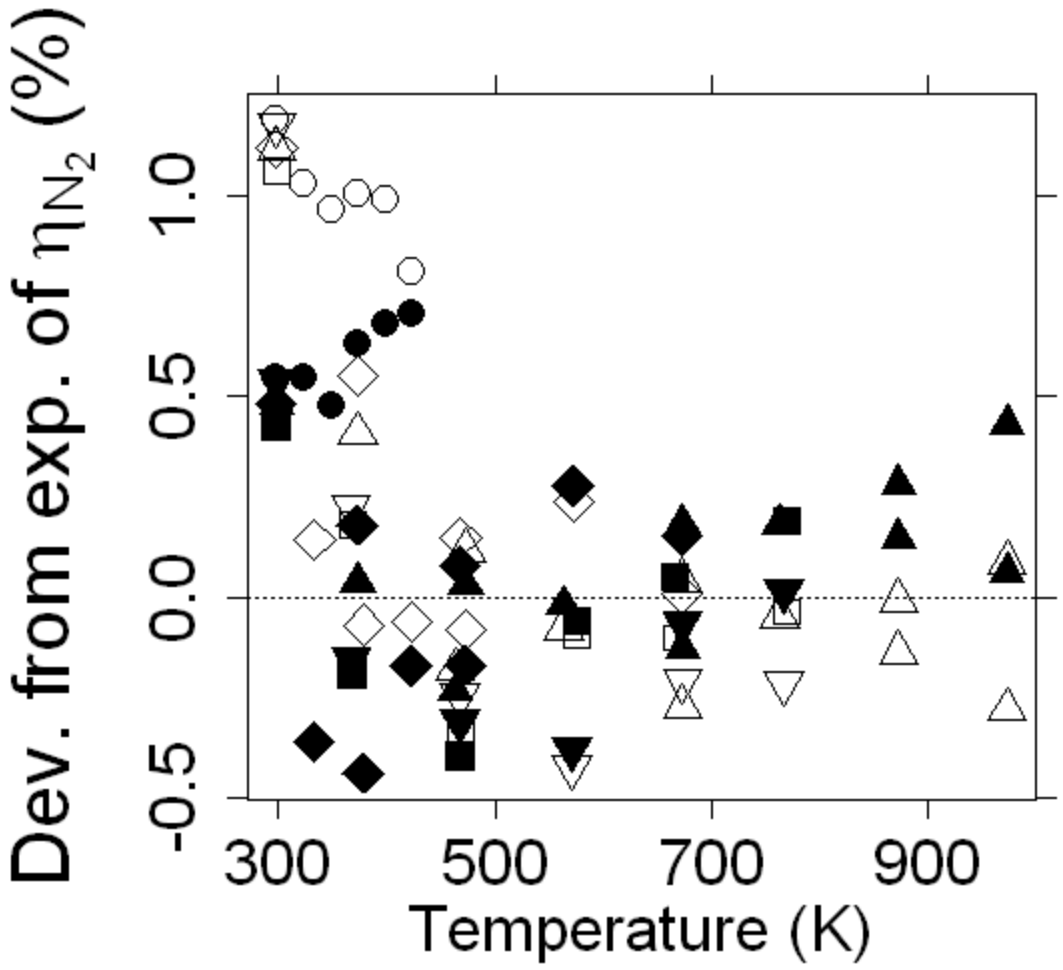

Figure 5: Deviation plot for differences between predicted and experimental viscosity of N_2.

MKC/DRFM: filled symbols. TRANLIB: unfilled symbols.

Experiments from: ○/●: Seibt et al. (2006) [36], ◇/◆: Kestin et al. (1977) [34], □/■: Helleman et al. (1973) [79], ▽/▼: Helleman et al. (1972) [80], △/▲: Kestin et al.(1972) [81] and [82].

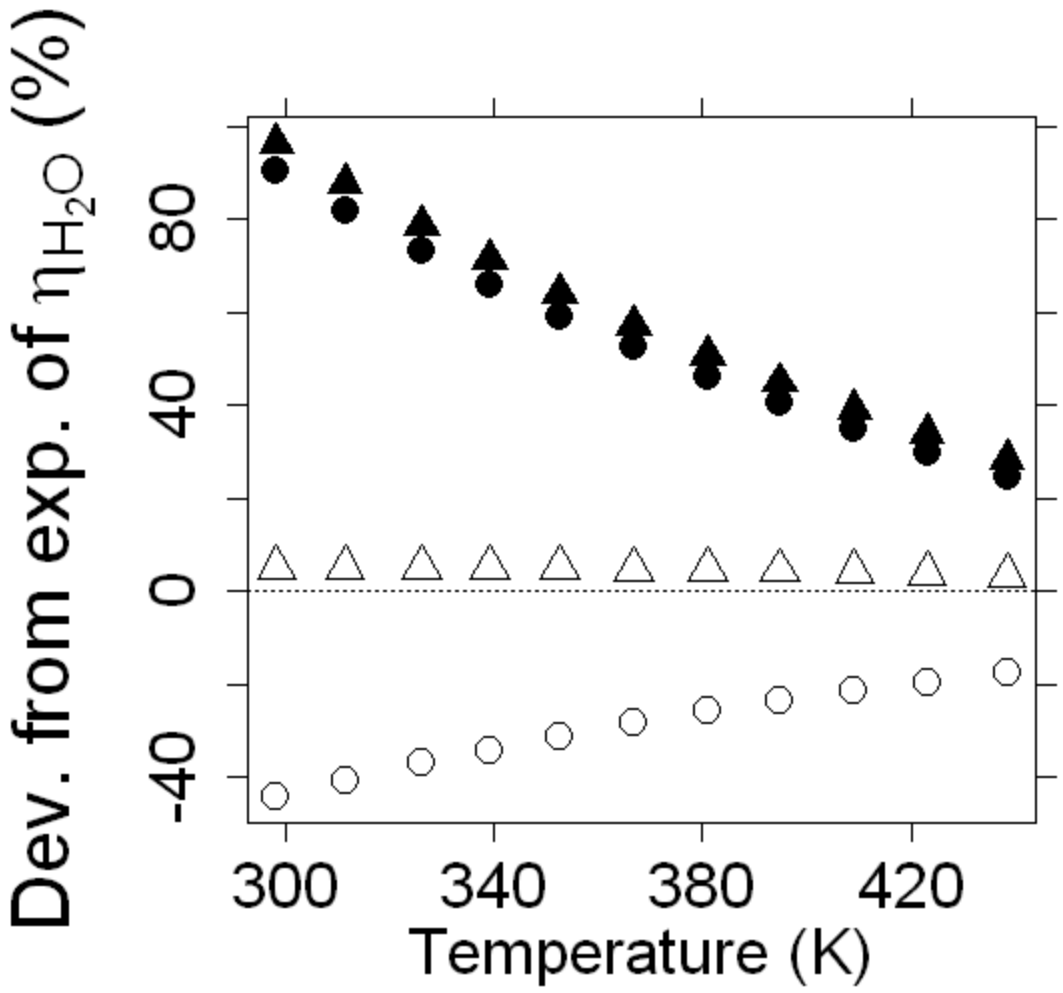

Figure 6: Deviation plot for differences between predicted and experimental H_2O viscosity for TRANLIB, DRFM, and MKC.

△ : TRANLIB. ▲ TRANLIB with dipole moment set to 0. ○: DRFM. ●: DRFM with dipole moment set to 0. See Table 6 for the potential parameters values used in the calculations.

Experiments are from [83].

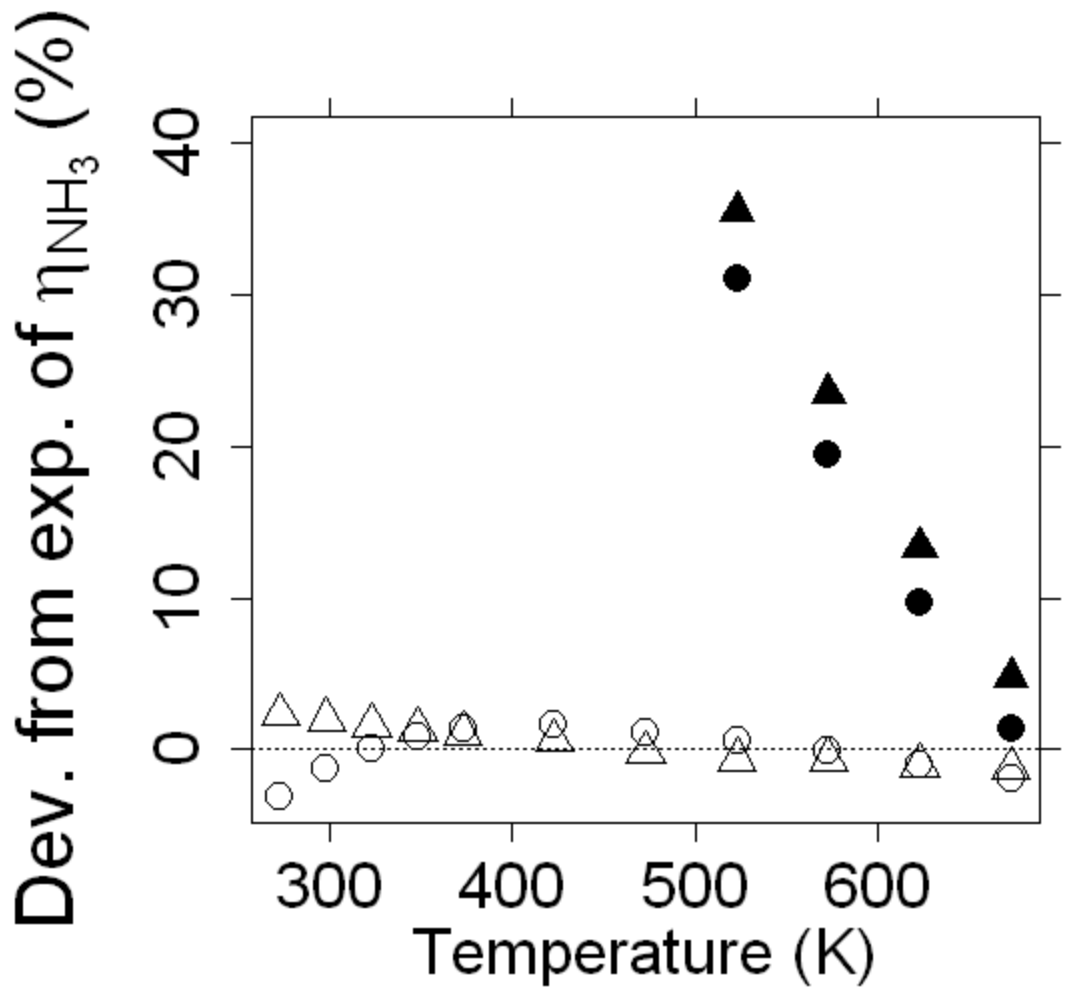

Figure 7: Deviation plot for difference between predicted and experimental viscosity of NH_3 as a function of temperature.

△ : TRANLIB. ▲ TRANLIB with dipole moment set to 0. ○: DRFM. ●: DRFM with dipole moment set to 0. See Table 6 for the potential parameters values used in the calculations.

Without polar correction, the deviations get so large at low temperatures that they are not shown on the plot.

Experiments are from [84].

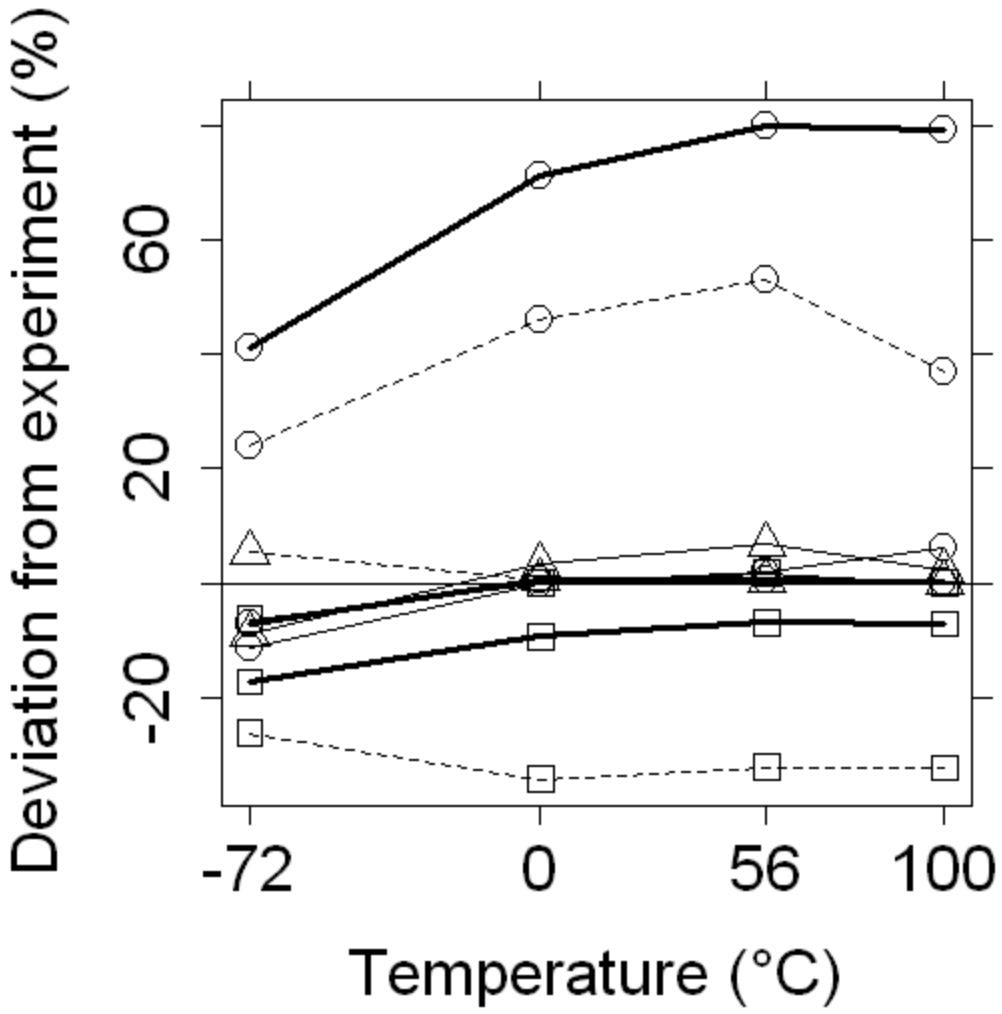

Figure 8: Deviation plot for differences between predicted viscosities of H atom, H_2 molecules, and H + H2 mixtures relative to experimental values.

Thick plain lines are TRANLIB, dashed lines are DRFM, and thin plain lines are the calculations by Cheng and Blackshear Jr. [67].

○ correspond to the viscosity of H. △ correspond to the viscosity of H_2 □ correspond to the interaction viscosity of H and H_2.

Experimental values by Cheng and Blackshear Jr. [67].

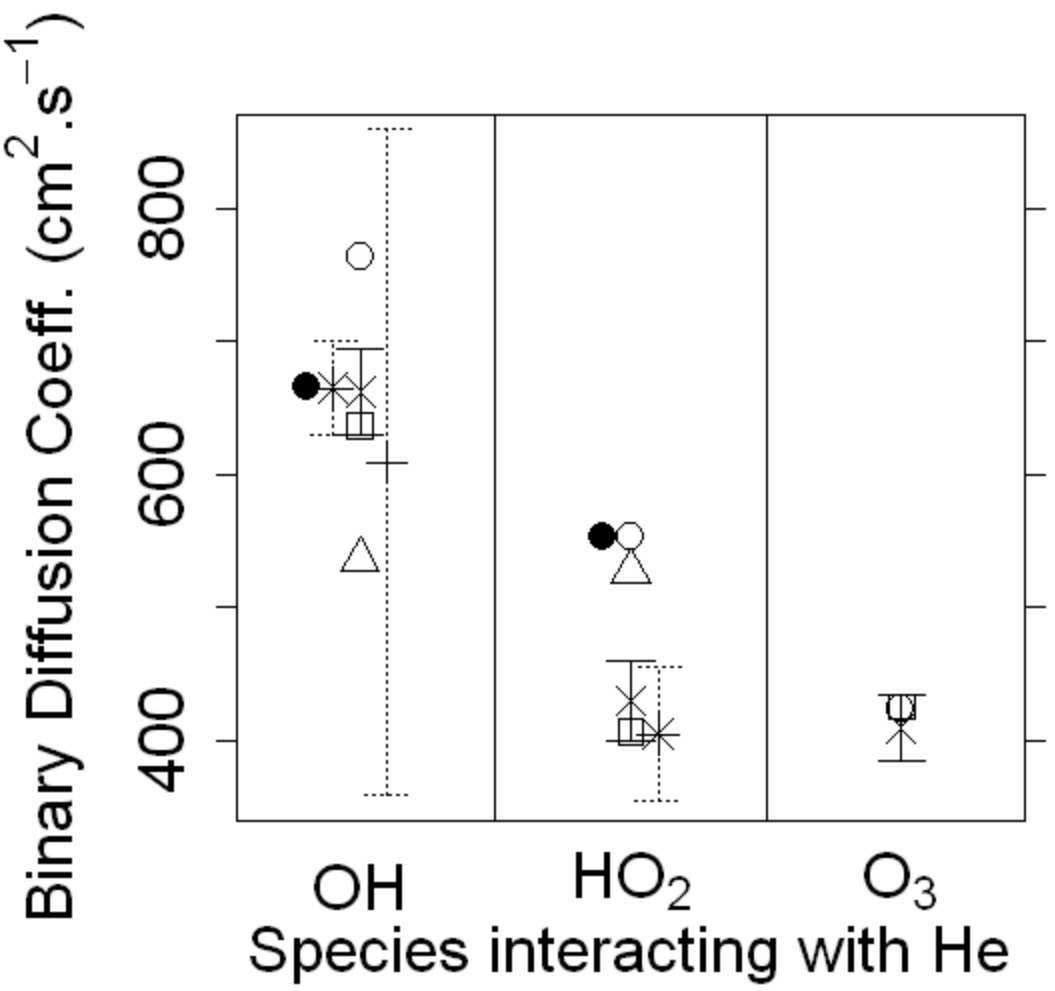

Figure 9: Binary diffusion coefficients for binary mixtures of He with three radical species measured and computed different ways.

The experimental values from Ivanov et al. (2007) are represented by × and the corresponding plain line denotes error bars. ○ indicates calculations by TRANLIB. Δ represents calculations by DRFM. □ is the calculation by Ivanov et al. (2007) . Binary mixture of He + OH: ∗ and its dotted line error bar corresponds to the experiment by Bertram et al. (2001) and + and its dotted line error bar corresponds to the experiment by Remorov et al. (1996). Binary mixture of He + HO_2: ∗ and its dotted line error bar corresponds to the experiment by Bedjanian et al. (2004). ●: values obtained with TRANLIB2 .

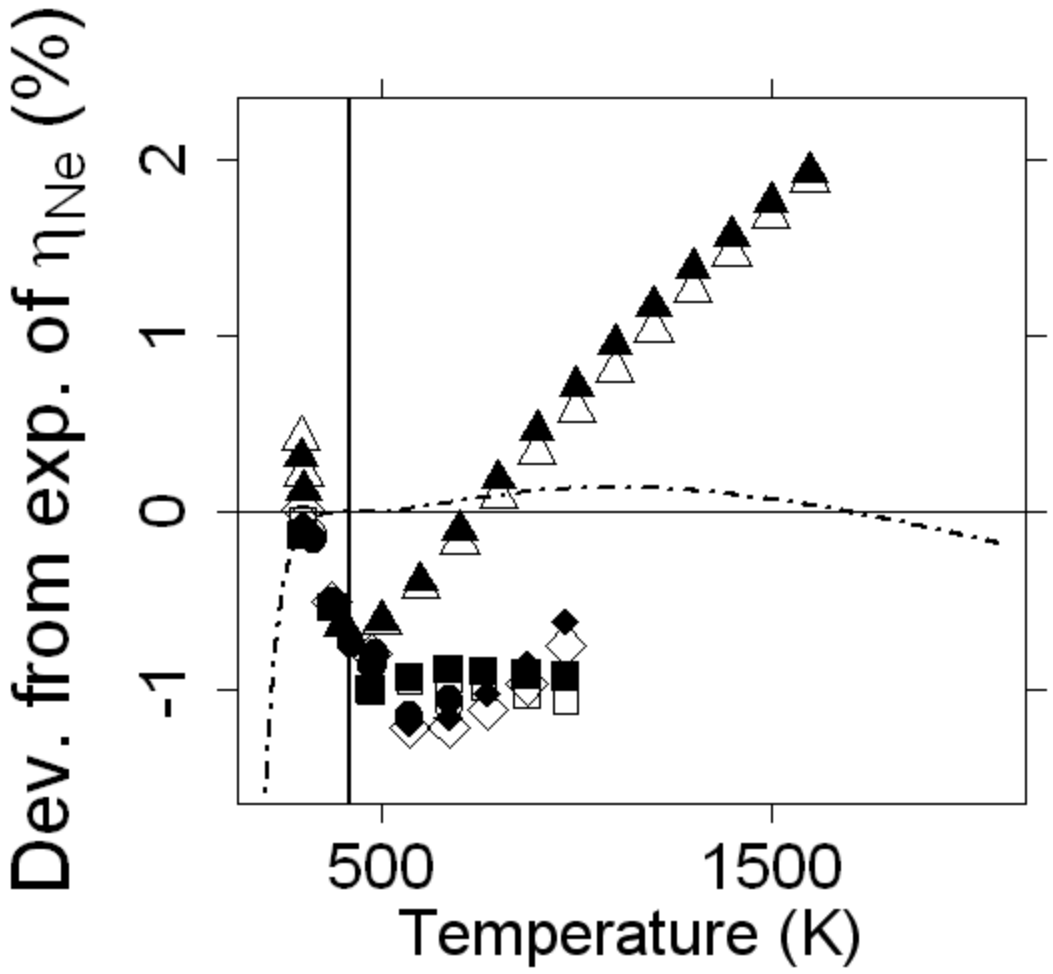

Figure 10: Deviation plot for differences between predicted (1st order) and experimental viscosity of Ne.

The unfilled symbols correspond to viscosities computed with the 2-parameter correlation. The filled symbols correspond to viscosities computed the 4-parameter correlation. The dots and dashes line corresponds to deviation between the two correlations (the 2-parameter one being the reference). The vertical line represents $T^* = 10$.

Experiments are from: ○/●: [34], △/▲:[85], □/■ : [86], and ◇/◆: [87].

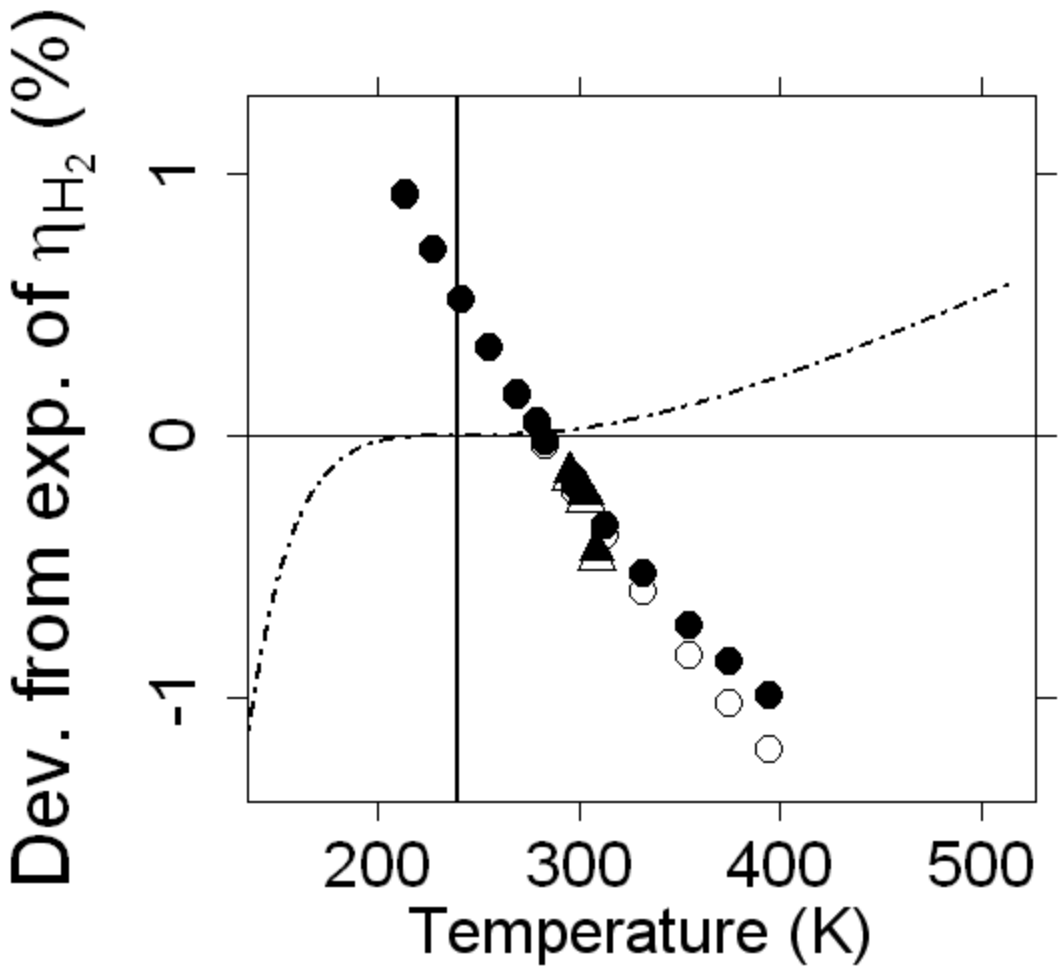

Figure 11: Deviation plot for differences between predicted (1st order) and experimental viscosity of H_2.

The unfilled symbols correspond to viscosities computed with the 2-parameter correlation. The filled symbols correspond to viscosities computed the 4-parameter correlation. The dots and dashes line corresponds to deviation between the two correlations (the 2-parameter one being the reference). The vertical line represents $T^* = 10$.

Experiments are from: ○/●: [88] and △/▲:[89].

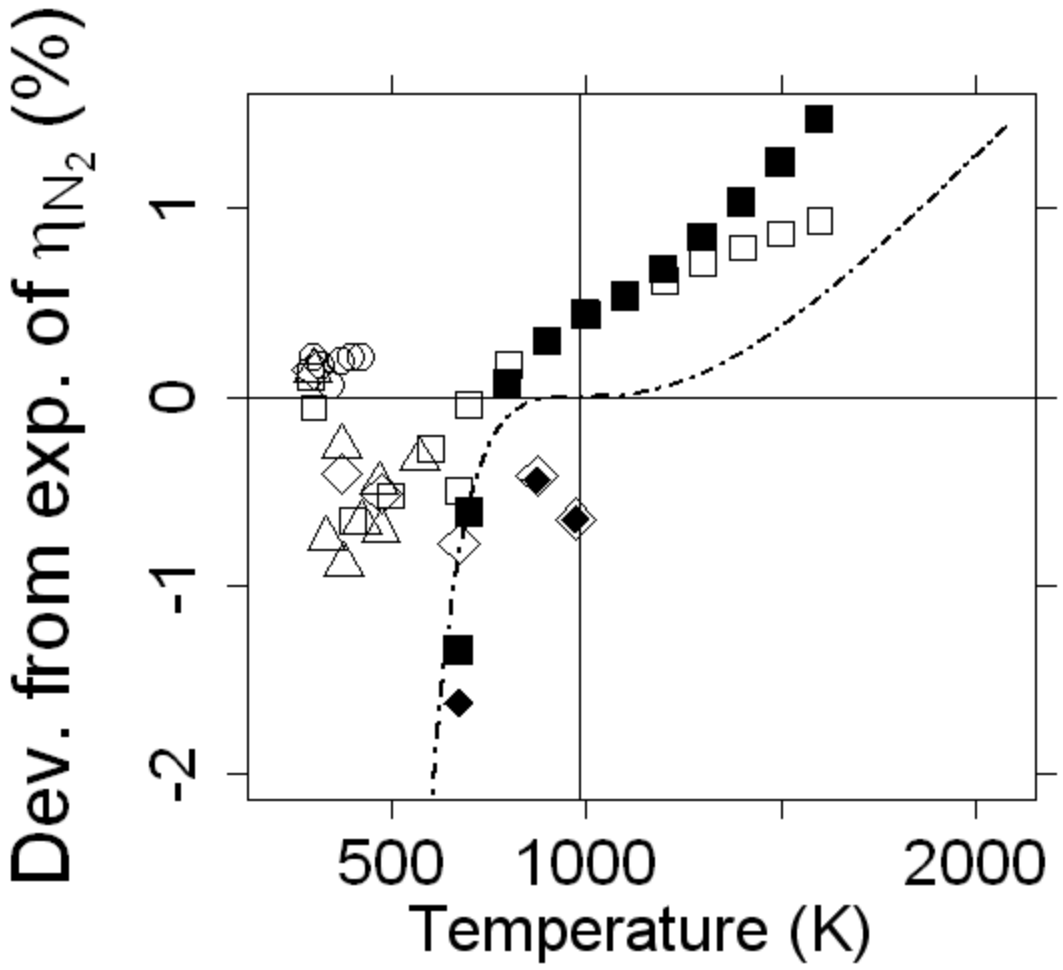

Figure 12: Deviation plot for differences between predicted (1st order) and experimental viscosity of N_2.

The unfilled symbols correspond to viscosities computed with the 2-parameter correlation. The filled symbols correspond to viscosities computed the 4-parameter correlation. The dots and dashes line corresponds to deviation between the two correlations (the 2-parameter one being the reference). The vertical line represents $T^* = 10$.

Experiments are from: ○/●: [36], △/▲: [34], □/■: [85], and ◇/◆: [81].

Figure 1

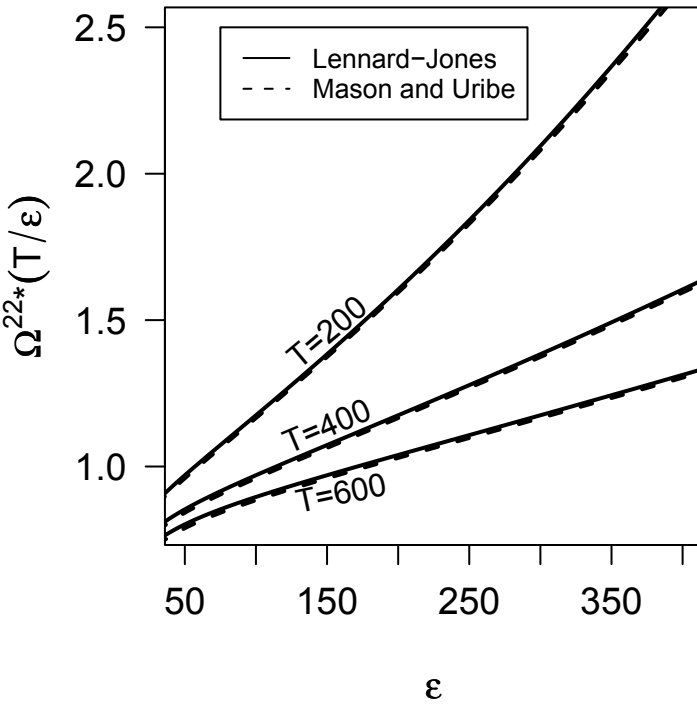
Lennard−Jones
Mason and Uribe
T=200
T=400
T=600
2.5
2.0
1.5
1.0
50
150
250
350
ε
Ω22*(T/ε)

Figure 2

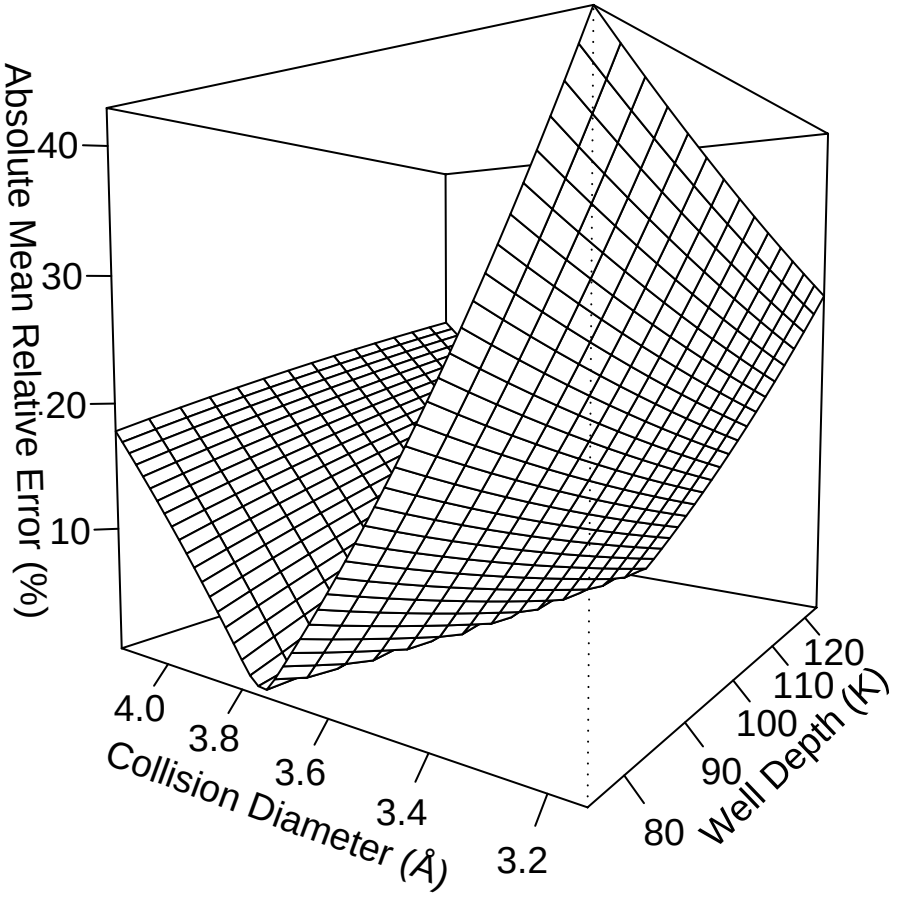
Absolute Mean Relative Error (%)
40
30
20
10
4.0
3.8
3.6
3.4
3.2
Collision Diameter (Å)
80
90
100
110
120
Well Depth (K)

Figure 3

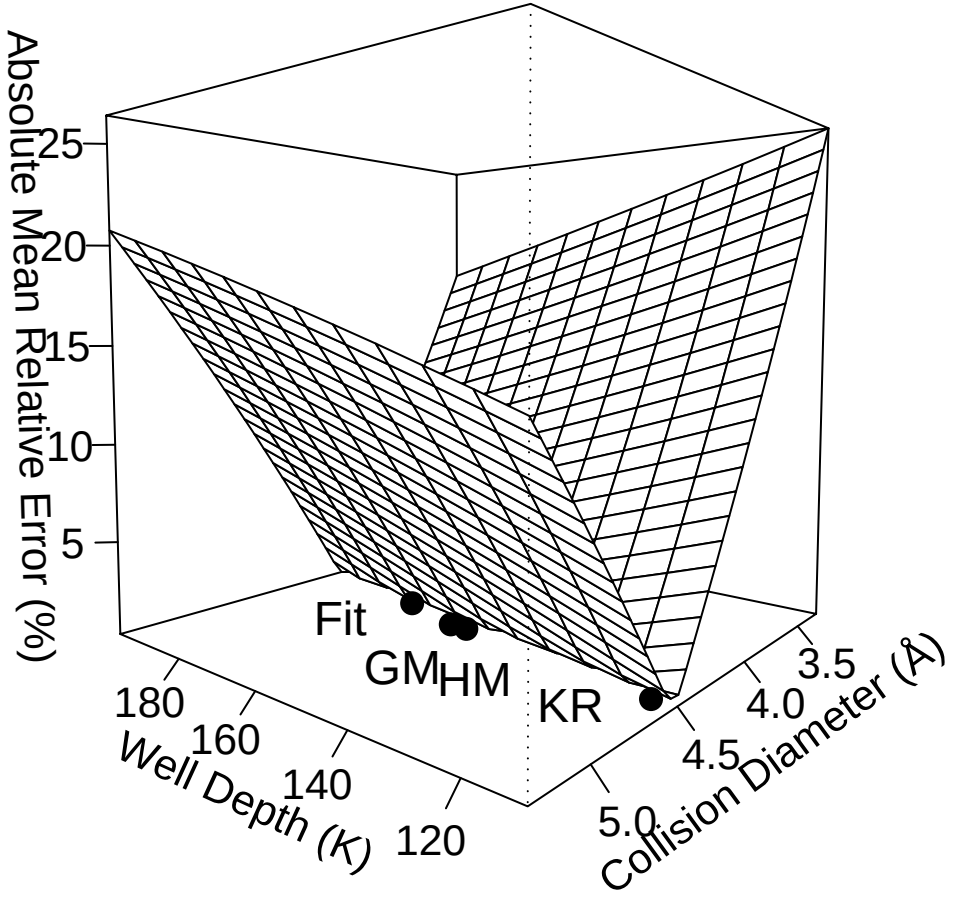
Absolute Mean Relative Error (%)
25
20
15
10
5
Fit
GM
HM
KR
180
160
140
120
Well Depth (K)
3.5
4.0
4.5
5.0
Collision Diameter (Å)

Figure 4

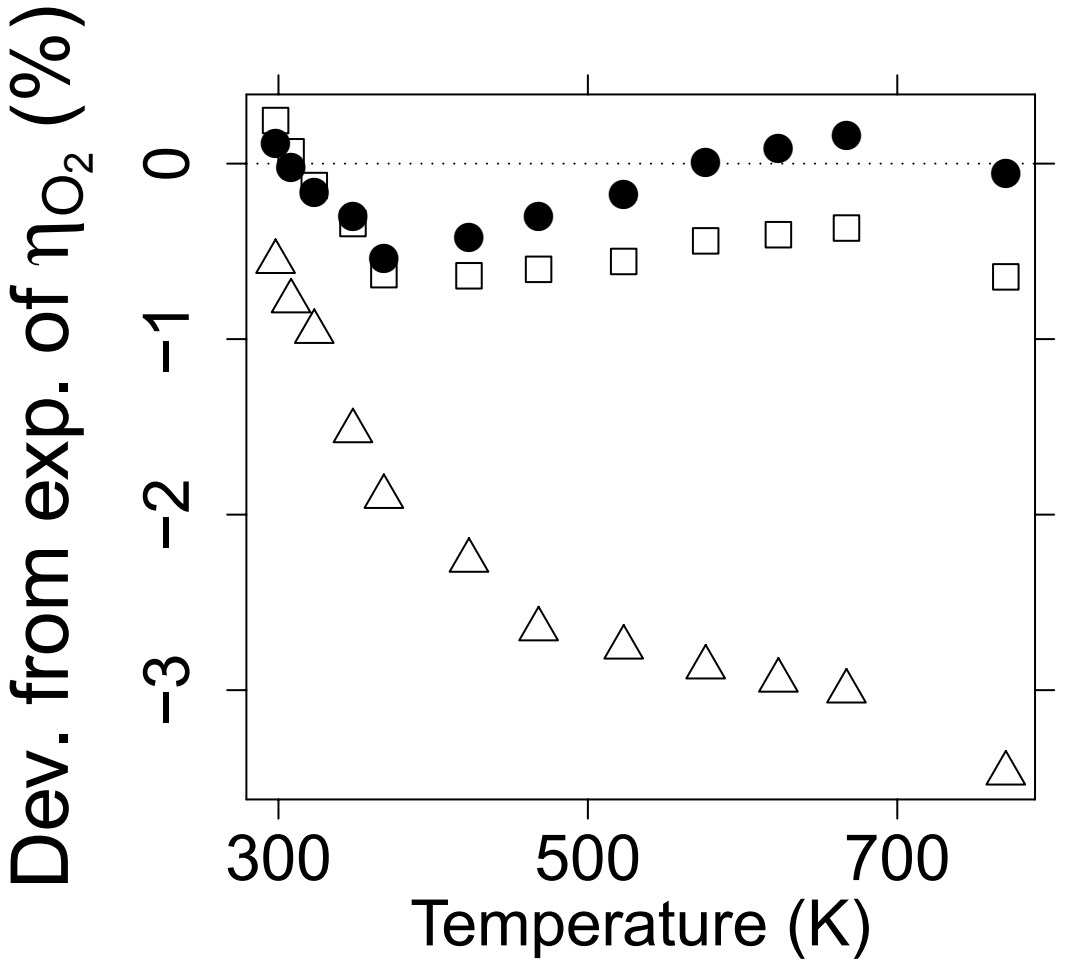

Figure 5

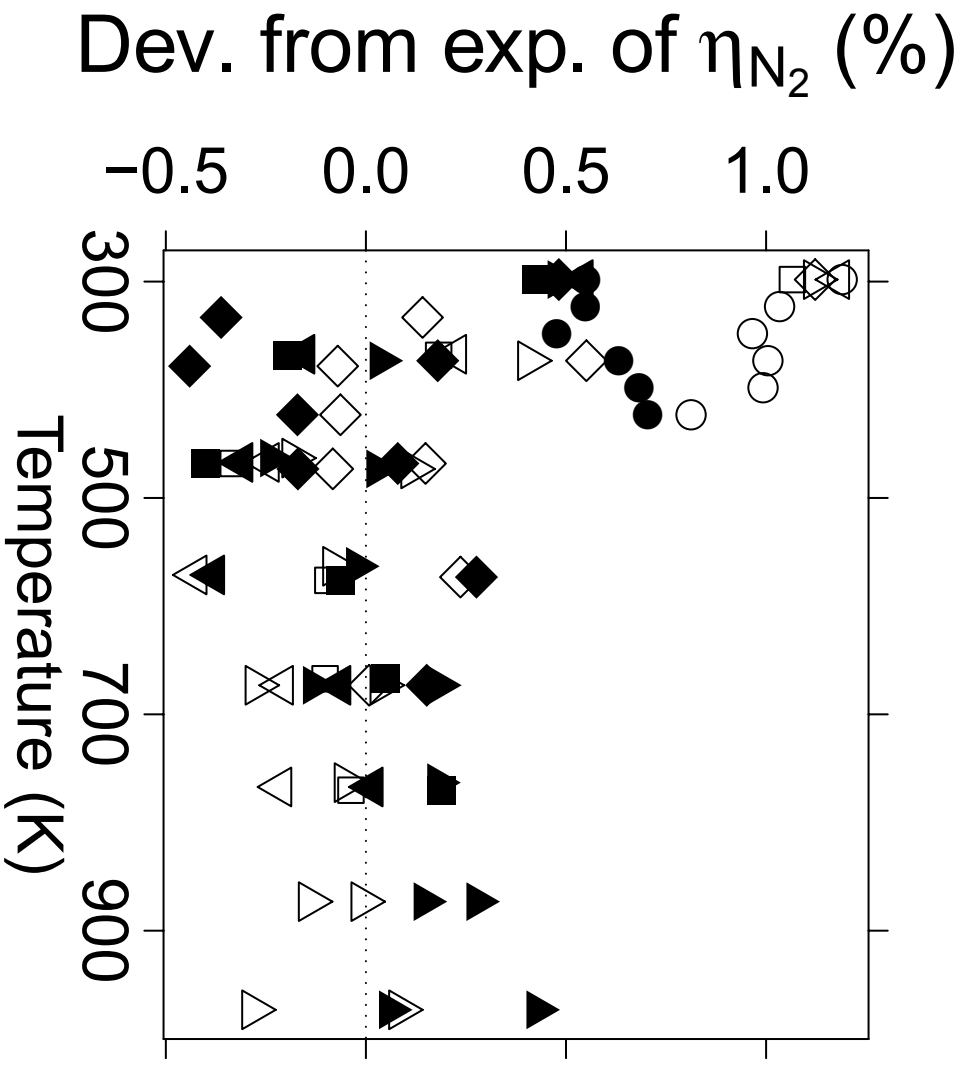

Figure 6

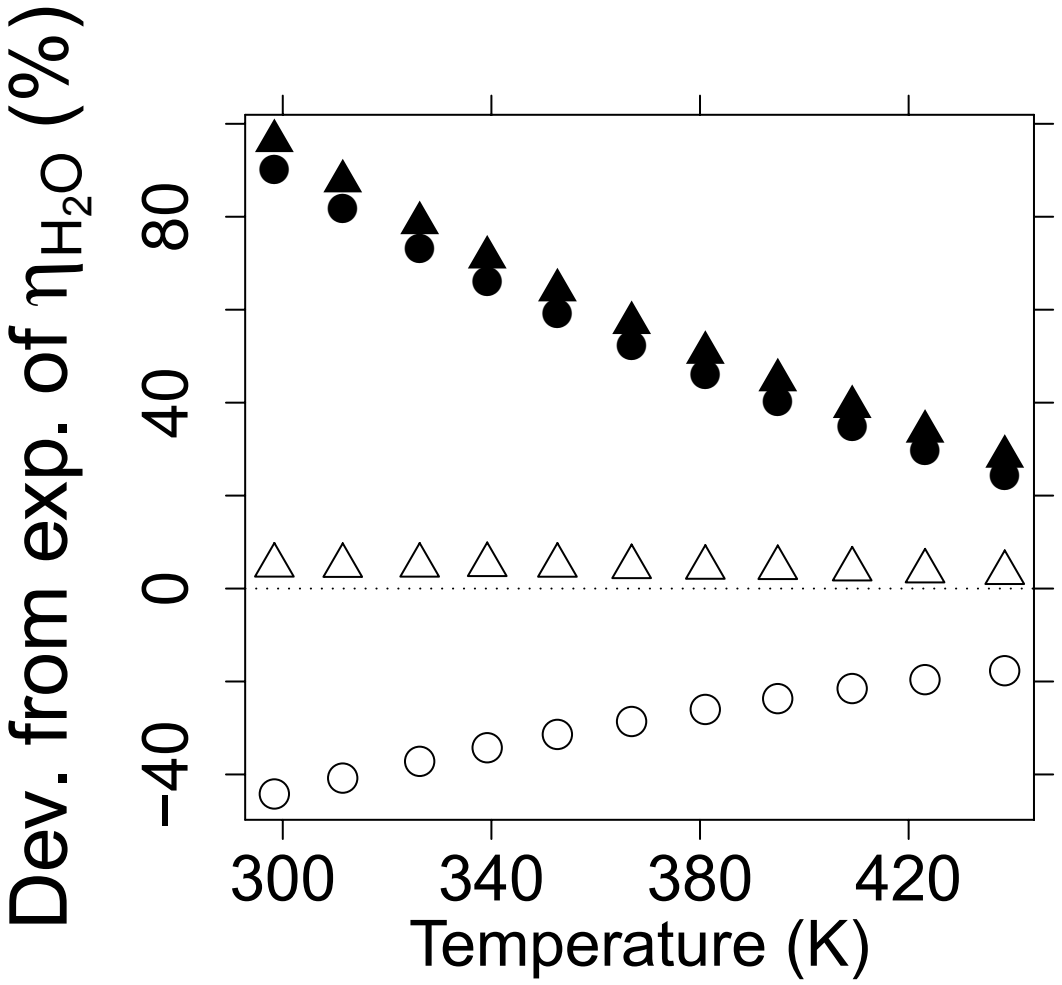

Figure 7

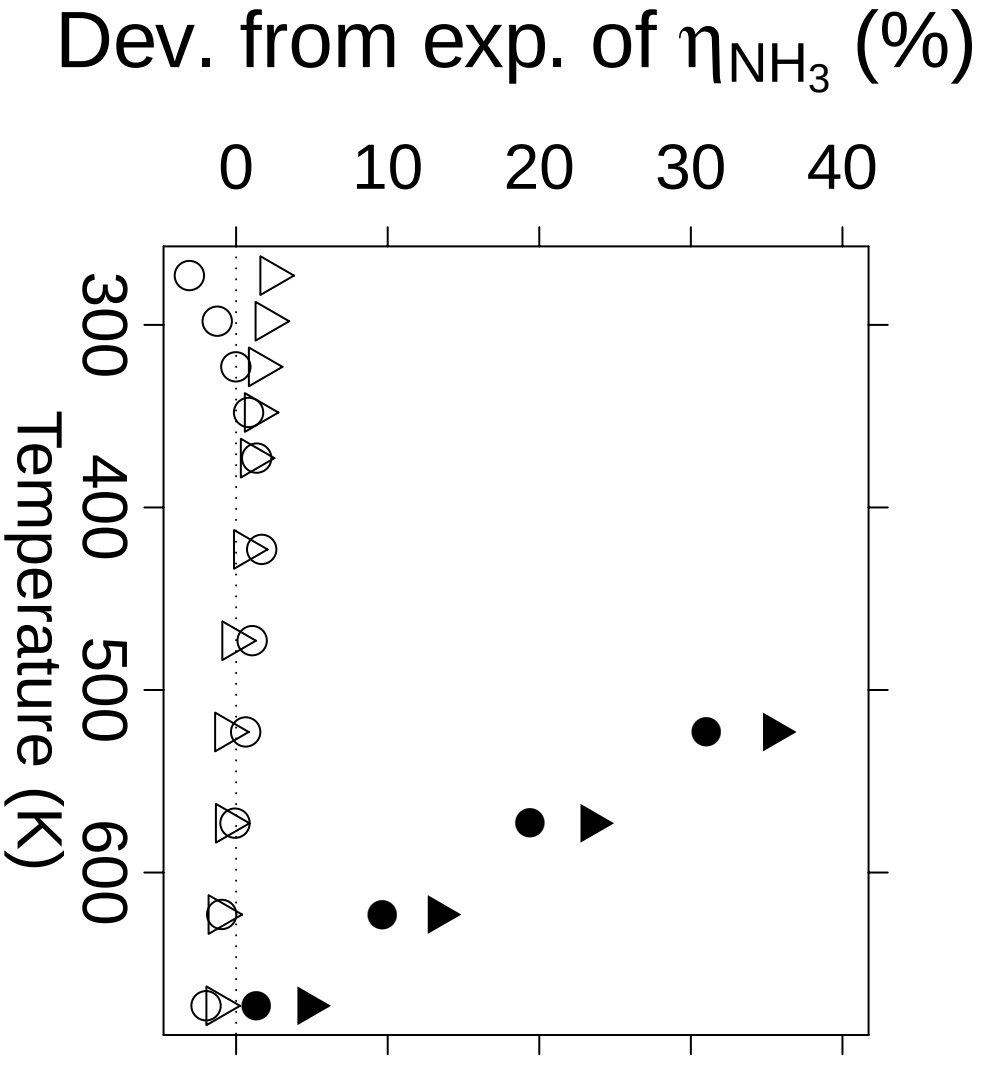
Dev. from exp. of η_{NH_3} (%)
0
10
20
30
40
Temperature (K)
300
400
500
600

Figure 8

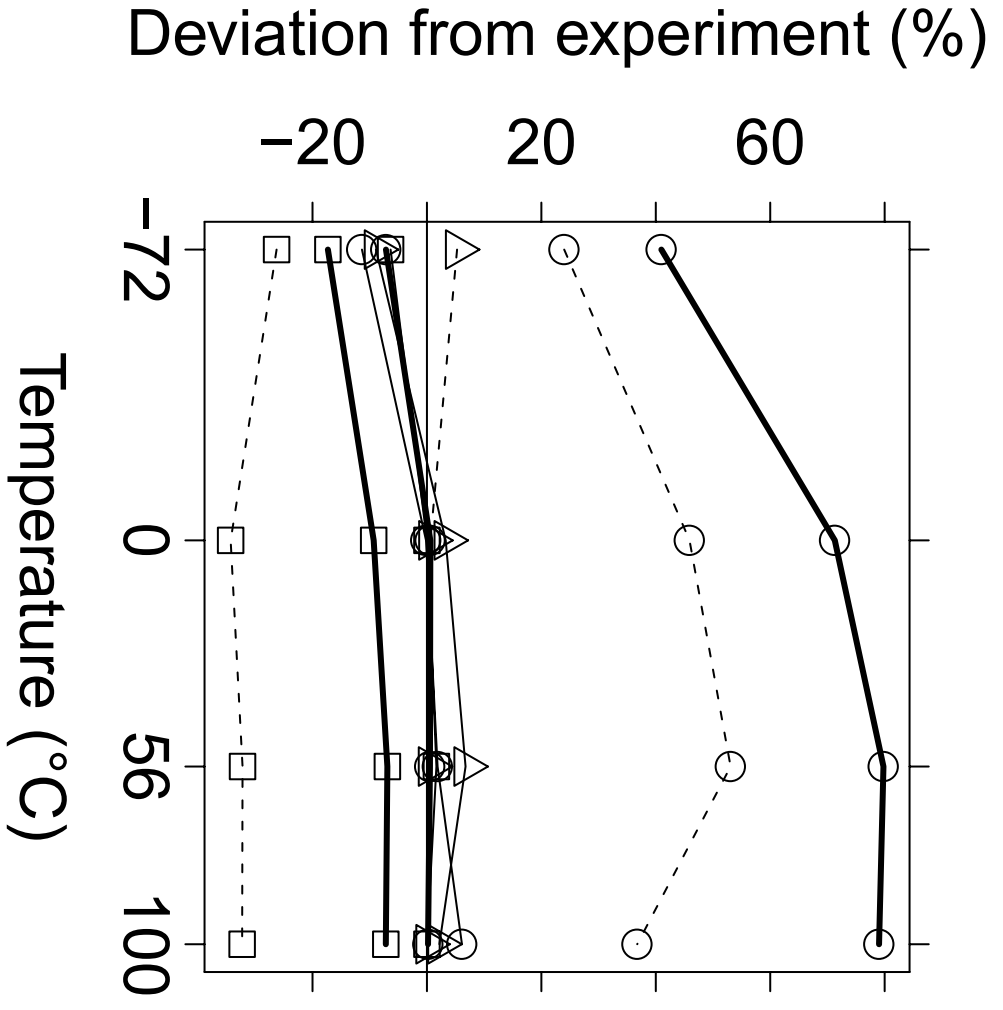

Figure 9

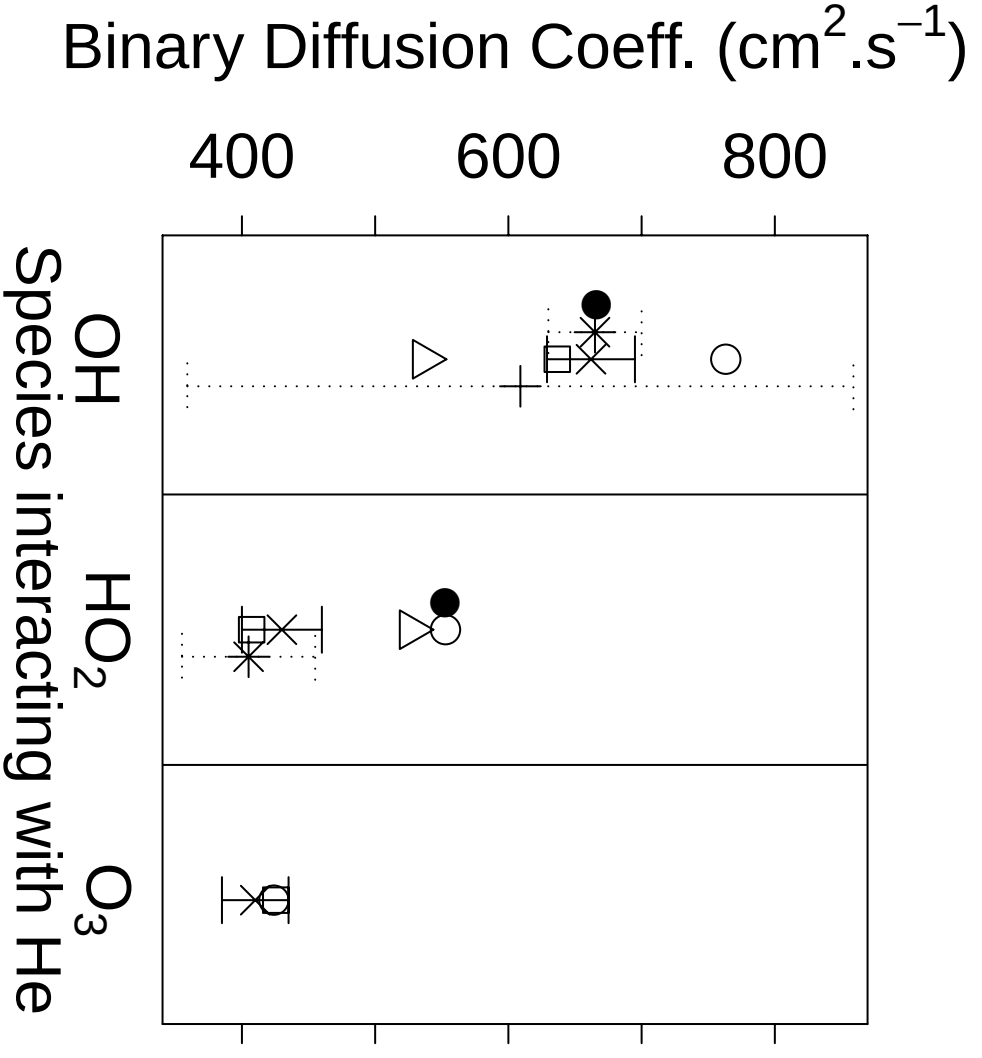
Binary Diffusion Coeff. ($cm^2.s^{-1}$)
400
600
800
Species interacting with He
OH
HO_2
O_3

Figure 10

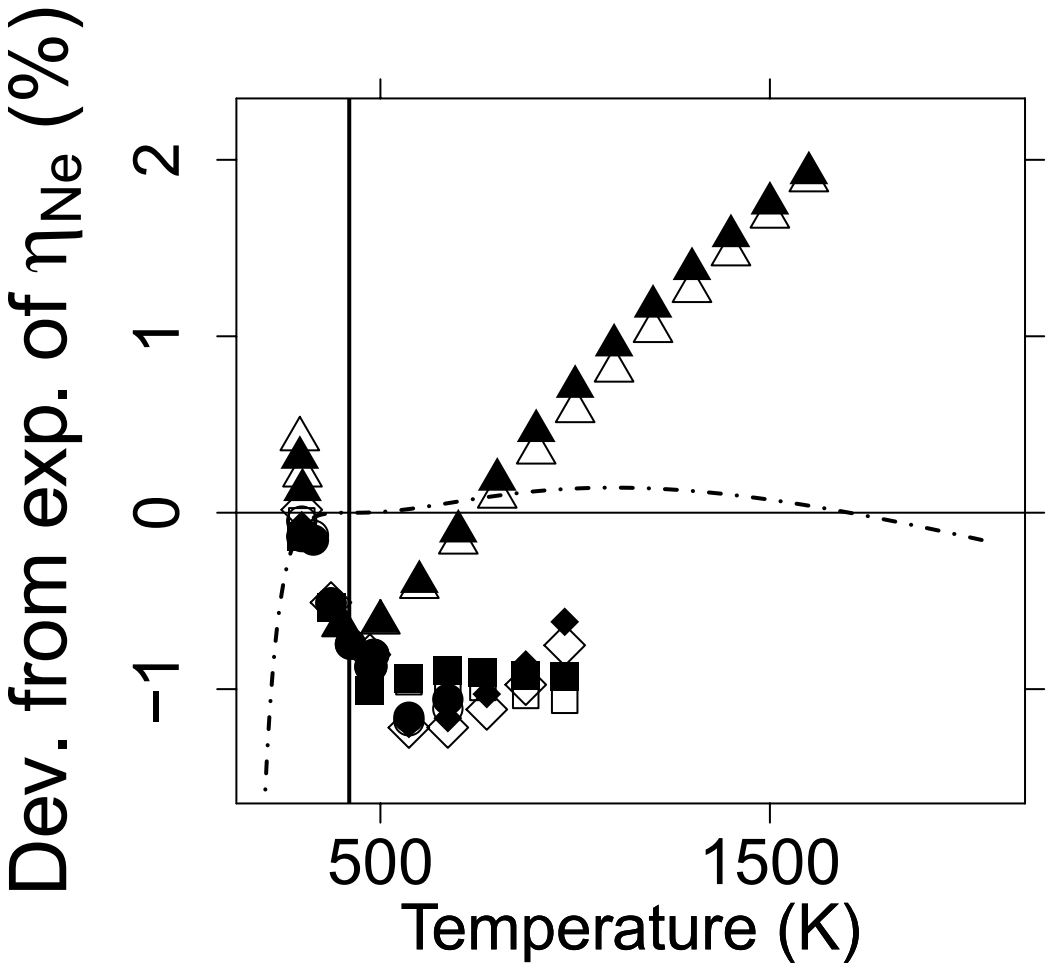

Figure 11

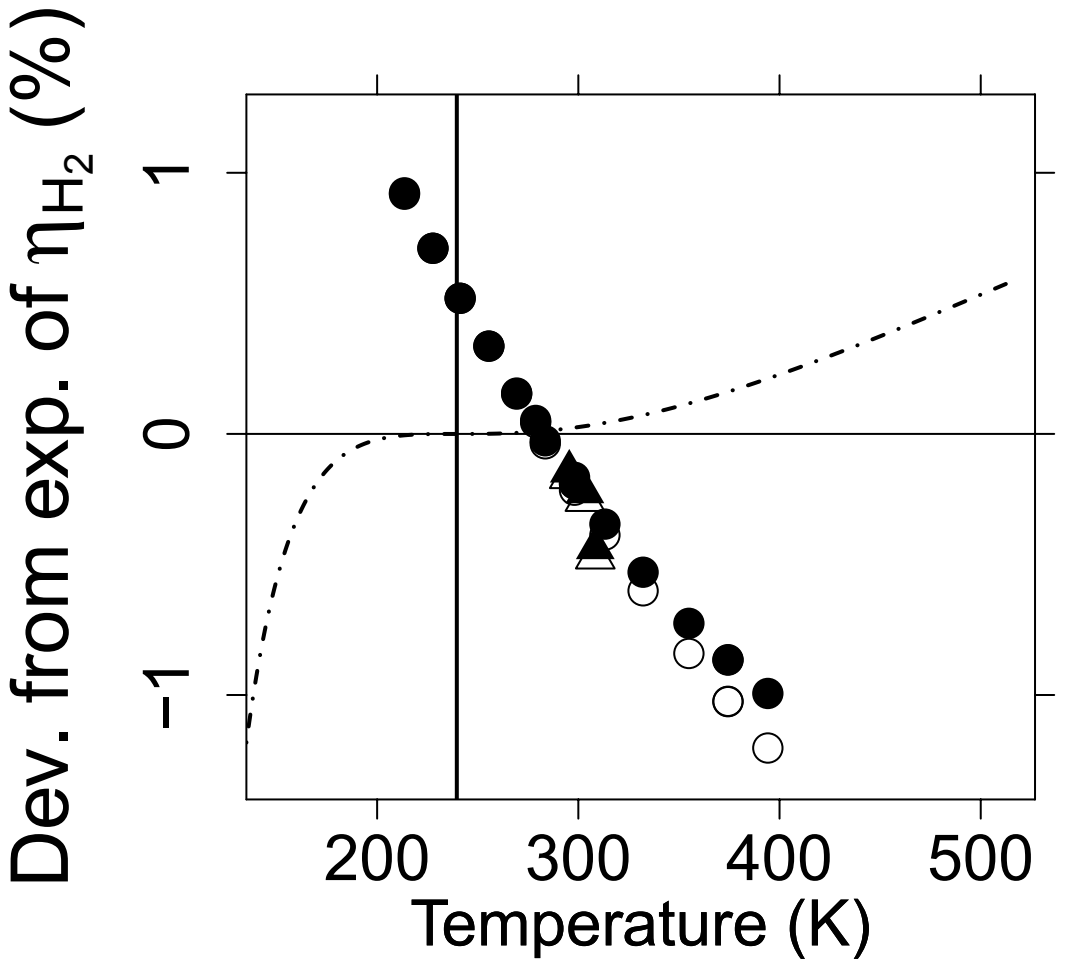

Figure 12

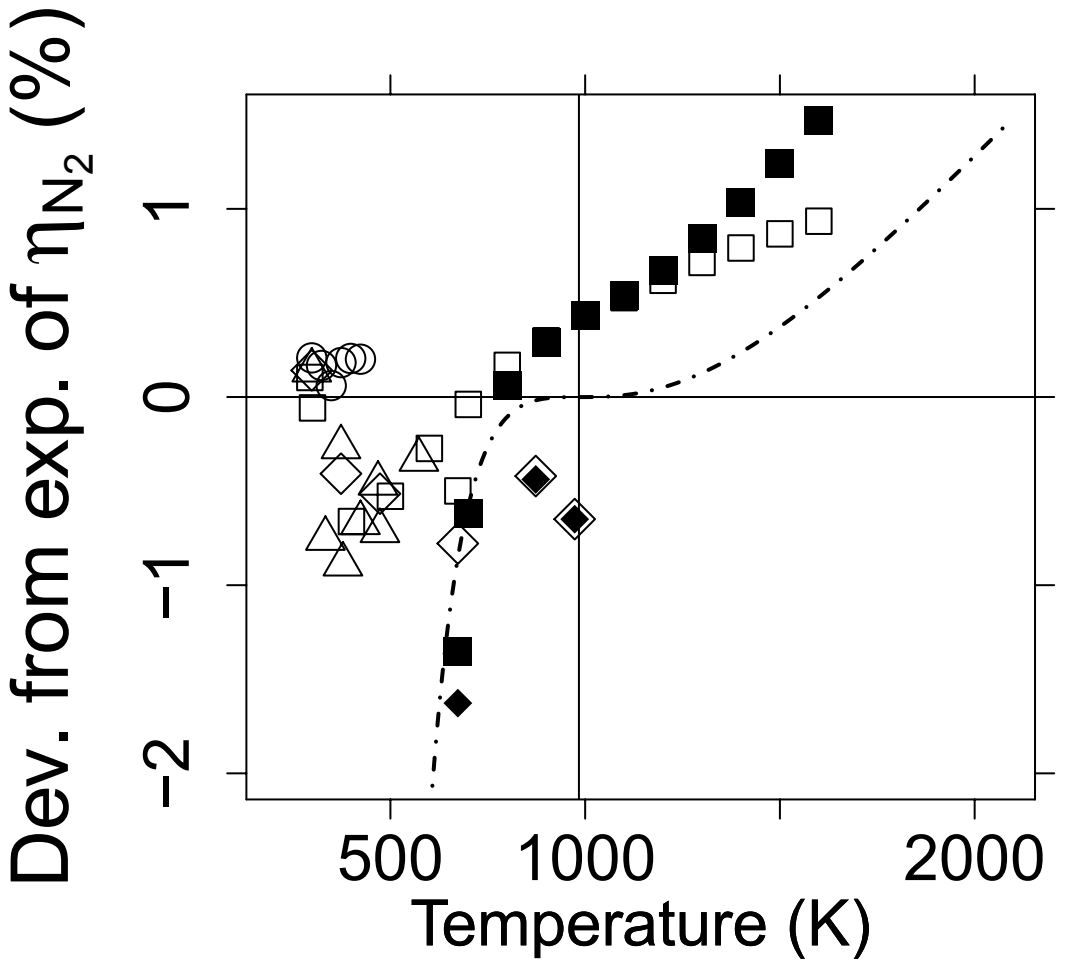

Table 1

i	a_{i1}	a_{i2}	b_{i1}	b_{i2}
1	0.18	0	0	0
2	0	0	0	0
3	-1.20407	-0.195866	10.0161	-10.5395
4	-9.86374	20.2221	-40.0394	46.0048
5	16.6295	-31.3613	44.3202	-53.0817
6	-6.73805	12.6611	-15.2912	18.8125

Table 2

i	a_i (noble and polyatomic gases)	b_i (noble gases)	b_i (polyatomic gases)
0	0.46641	0.357588	0.295402
1	-0.56991	-0.472513	-0.510069
2	0.19591	0.0700902	0.189395
3	-0.03879	0.016574	-0.045427
4	0.00259	-0.00592022	0.0037928

Table 3

i	a_{i1}	a_{i2}	a_{i3}	a_{i4}	
1	-33.0838	20.0862	72.1052	8.27648	
2	101.571	56.4472	286.393	17.7610	
3	-87.7036	46.3130	277.146	19.0573	
i	b_{i1}	b_{i2}	b_{i3}	b_{i4}	c_i
2	-267.00	201.570	174.672	7.36916	1
4	26700	-19.2265	-27.6938	-3.2955	10^3
6	-8.9×10^5	6.31013	10.2266	2.33033	10^5

Table 4

	ε (K)		σ (Å)	
	TRANLIB	DRFM	TRANLIB	DRFM
Ar	136.500	143.20	3.330	3.350
O_2	107.400	121.1	3.458	3.407
N_2	97.530	98.4	3.621	3.652
CO_2	244.000	245.3	3.763	3.769
CH_4	141.400	161.4	3.746	3.721
H_2O	572.400	535.21	2.605	2.673
NH_3	481.000	282.2[1]	2.290	3.30[1]
HO_2	107.400	365.56	3.458	3.433
OH	80.000	281.27	2.750	3.111
H_2O_2	107.400	368.11	3.458	3.499

[1] Fitted values

Table 5

	μ (Debye)		α (Å^3)	
	TRANLIB	DRFM	TRANLIB	DRFM
Ar	0.000	0	0.000	1.642
O_2	0.000	0	1.600	1.600
N_2	0.000	0	4.000	1.750
CO_2	0.000	0	2.650	2.65
CH_4	0.000	0	2.600	2.60
H_2O	1.844	1.847	0.000	1.450
NH_3	1.470	1.4718[1]	0.000	2.81[1]
HO_2	0.000	2.09	0.000	1.950
OH	0.000	1.655	0.000	0.980
H_2O_2	0.000	1.573	0.000	2.230

[1] Value taken from reference [66]

Table 6

		ε (K)	σ (Å)	μ (Debye)	α (Å^3)
H_2O	TRANLIB	572.4	2.61	1.844	0
	TRANLIB, without polar correction	572.4	2.61	0	0
	DRFM	535.2	2.67	1.847	1.45
	DRFM, without polar correction	535.2	2.67	0	0
NH_3	TRANLIB	481.0	2.92	1.47	0
	TRANLIB, without polar correction	481.0	2.92	0	0
	DRFM	282.2[1]	3.30[1]	1.4718[2]	0.281[2]
	DRFM, without polar correction	282.2	3.30	0	0

[1] Fitted value
[2] Value taken from reference [66]

Table 7

	OH and He	HO_2 and He	O_3 and He
TRANLIB	673.4	553.0	424.2
DRFM	636.7	526.9	X
Measured by Ivanov et al (2007) [69]	662 ± 33	430 ± 30	410 ± 25
Computed by Ivanov et al (2007) [69]	636.7	407.3	425.4
From Remorov et al. (1996) [70]	609 ± 250	X	X
From Bertram et al. (2001) [71]	665 ± 35	X	X
From Bedjanian et al. (2004) [72]	X	405 ± 50	X
TRANLIB2	666.3	552.6	X

Table 8

		ε (K)	σ (Å)	α (Å^3)	μ (Debye)
OH	TRANLIB	80.000	2.750	0.000	0.000
	TRANLIB2	572.40	2.605	0.98	1.74
	DRFM	281.27	3.111	0.980	1.655
	Ivanov et al (2007) [69]	809.1	2.641	X	1.74
He	TRANLIB	10.200	2.576	0.000	0.000
	TRANLIB2	10.200	2.576	0.200	0.000
	DRFM	10.40	2.610	0.200	0
	Ivanov et al (2007)	10.22	2.556	X	0
HO_2	TRANLIB	107.400	3.458	0.000	0.000
	TRANLIB2	107.400	3.458	1.95	2.090
	DRFM	356.56	3.433	1.950	2.09
	Ivanov et al (2007)	298.3	4.196	X	2.090
O_3	TRANLIB	180.000	4.100	0.000	0.000
	DRFM	X	X	X	X
	Ivanov et al (2007)	106.7	3.467	X	0